17 Beyond Quark Flavor Physics

17.1 General View

17.1.1 Preliminaries

Until now this book has been dominated by quark flavor-violating processes. Yet in the search for NP it is crucial to consider other phenomena and observables. Here in particular

- Charged lepton violation (LFV),
- Electric dipole moments of the nucleons, atoms, molecules, and leptons (EDMs),
- Anomalous magnetic moments of leptons $a_\ell = \frac{1}{2}(g-2)_\ell$ with $\ell = e, \mu, \tau$, and
- Neutrino oscillations and neutrinoless double β decay

play important roles. Therefore, this chapter will be devoted to the these topics, although our presentation will not be as detailed as was the case of previous chapters not only because the author worked less on lepton flavor physics than quark flavor physics but also because some of the relevant experiments are not as advanced as is the case of those studying meson decays. But as we will see in the case of LFV and EDMs, the contributions from the SM dynamics being very small cannot be measured even in the next decade, and the observation of any positive signal would be a clear evidence for NP. In this respect they differ profoundly from all processes discussed by us until now, which suffer from a large background coming from the SM, and one needs precise theory and precise experiment to identify NP. In the case of LFV and EDMs, theoretical uncertainties by a factor of two still do not matter even if present upper experimental bounds on various observables put already now significant constraints on the parameters of NP models.

The case of $(g-2)_\mu$ is different. On the one hand, the Brookhaven measurement [1115], at the beginning of this millennium, exhibited a significant departure from SM expectations. But the presence of hadronic uncertainties and the fact that only one experiment has seen this anomaly do not allow to make yet firm conclusions whether NP has been seen here or not. The new experiment at Fermilab and persistent efforts by theorists should improve this situation in the coming years. An experiment at J-PARC should provide an independent measurement in the coming years.

Concerning the last item on our list, the observation of neutrino oscillations is a clear signal of physics beyond the SM and so far together with dark matter and matter-antimatter asymmetry observed in our universe the only clear signal of NP. In principle, we could devote one section to this topic in this book. But as in this case, there are already books

Downloaded from https://www.cambridge.org/core. UNIVERSIDAD AUTONOMA METROPOLITANA, on 16 Nov 2026 at 21:17:32, subject to the Cambridge Core terms of use, available at https://www.cambridge.org/core/terms. https://doi.org/10.1017/9781139524100.023

devoted entirely to this topic, in particular [23], we will only make a few comments and refer to recent reviews.

In the course of our presentation we will frequently refer to the literature. As these four topics are often discussed together, it is useful to refer already now to selected reviews on them, which can be found in [803, 1116–1121]. Many references to the original literature can be found there. Moreover, the study of correlations between LFV, $(g-2)_\mu$, and EDMs in supersymmetric flavor models and SUSY GUTS can be found in [529, 1003, 1122, 1123]. Analogous correlations in models with vector-like leptons have been presented in [1039], and general expressions for these observables in terms of Wilson coefficients of dimension-6 operators can be found in [795]. We will encounter some of these expressions later.

17.1.2 General Considerations

Before going into mathematical details in the next sections, it is useful to discuss certain properties of the topics in question, as in concrete models there exist definite correlations between the observables representing them. But fortunately for us these correlations are model dependent, and studying them one can learn about the dynamics at very short distance scales in a manner we did already in the case of quark flavor physics.

To illustrate it on a concrete example, let us consider first

$$\mathcal{B}(\mu \to e\gamma), \qquad \mathcal{B}(\mu \to 3e), \qquad T(\mu N \to eN), \qquad d_e, \qquad a_e, \tag{17.1}$$

with the last three representing, respectively, the $\mu \to e$ conversion in nuclei, electric dipole moment of the electron, and its anomalous magnetic moment.

In general, a given interaction can be CP-violating, CP-conserving, flavor-violating, and flavor-conserving. Moreover, the operator structure governing the observables just listed can be model dependent. We note in particular the following features that will be seen explicitly in the formulas presented in the next sections.

- The decay $\mu \to e\gamma$ requires lepton flavor-violation, which could be accompanied by CP-violating phases but could also take place without them. Moreover, similar to $b \to s\gamma$ decay, this transition is fully dominated by dipole operators.
- The decay $\mu \to 3e$ and the transition $\mu N \to eN$ require, similar to $\mu \to e\gamma$, LFV with or without CP-violating phases but are not necessarily fully dominated by dipole operators. Box diagrams and penguin diagrams of various sorts can also give important contributions in certain NP scenarios.
- The electric dipole moment d_e requires CP-violating sources but can proceed without flavor violation. The dipole operator is the prime source here.
- The anomalous magnetic moment a_e does not require any CPV and LFV in contrast to the remaining observables considered here. Similar to $\mu \to e\gamma$ and d_e, it is governed by dipole operators.

These different properties demonstrate that the correlations between observables in (17.1) must be model dependent. This is clearly seen in the correlation between d_e and a_e, both governed by dipole operators and both being flavor conserving [1124]

Downloaded from https://www.cambridge.org/core. UNIVERSIDAD AUTONOMA METROPOLITANA, on 16 Nov 2026 at 21:17:32, subject to the Cambridge Core terms of use, available at https://www.cambridge.org/core/terms. https://doi.org/10.1017/9781139524100.023

$$d_e(\mathrm{NP}) = a_e(\mathrm{NP})\frac{e}{2m_e}\tan\phi_e^{\mathrm{NP}}, \tag{17.2}$$

with ϕ_e^{NP} being a model-dependent NP phase.

To study flavor structure of a given model, it is crucial to study in addition decays like $\tau \to \mu\gamma$, $\tau \to 3\mu$, and alike. Moreover, in certain cases the mechanism for generation of neutrino masses can bring along new dynamics causing observable transitions listed earlier.

One should stress that although no EDM of any particle has been measured so far and no charged lepton flavor violation has been observed, the 2020s should bring spectacular advances in the increased sensitivity of many observables considered in the next sections, providing thereby a window to the dynamics well above the scales explored by the LHC. We summarize the present upper bounds and experimental prospects for LFV in Tables 17.1 and 17.2 and for EDMs in Table 17.7

17.1.3 Spin-1/2 Electromagnetic Formfactors

It is instructive to write down the matrix elements of the electromagnetic current

$$J_\mu^{em} = e\sum_f Q_f \bar{f}\gamma_\mu f \tag{17.3}$$

that are relevant for the discussion of magnetic and electric dipole moments as well as electromagnetic transition dipole moments responsible for $\mu \to e\gamma$ decay and related decays like $\tau \to \mu\gamma$ and $\tau \to e\gamma$. We follow here [1124].

We have first

$$\langle f(p')|J_\mu^{em}|f(p)\rangle = \bar{u}_f(p')\Gamma_\mu u_f(p), \tag{17.4}$$

with f being an arbitrary spin-1/2 fermion with initial momentum p and final momentum p' so that $q = p' - p$. $\bar{u}_f$ and u_f are Dirac spinors. Assuming Lorentz invariance and taking into account the hermiticity of J_μ^{em}, one has

$$\Gamma_\mu = F_1(q^2)\gamma_\mu + iF_2(q^2)\sigma_{\mu\nu}q^\nu - F_3(q^2)\sigma_{\mu\nu}q^\nu\gamma_5 + F_A(q^2)(\gamma_\mu q^2 - 2m_f q_\mu)\gamma_5, \tag{17.5}$$

with the formfactors $F_i(q^2)$ being real. The first three formfactors are the charge, anomalous magnetic dipole, and electric dipole formfactors. At $q^2 = 0$ we have then

$$F_1(0) = Q_f e = \text{electric charge}, \tag{17.6}$$

$$F_2(0) = a_f Q_f \frac{e}{2m_f} = \text{anomalous magnetic moment}, \tag{17.7}$$

$$F_3(0) = d_f Q_f = \text{electric dipole moment}. \tag{17.8}$$

For neutral particles the last two parametrizations are not useful and one can use as done in [1124] $Q_f \to 1$ for neutron and $Q_f \to -1$ for neutrino. But other choices are possible. $F_A(q^2)$ is called anapole formfactor. It is usual related to electroweak loop effects, and we

Downloaded from https://www.cambridge.org/core. UNIVERSIDAD AUTONOMA METROPOLITANA, on 16 Nov 2026 at 21:17:32, subject to the Cambridge Core terms of use, available at https://www.cambridge.org/core/terms. https://doi.org/10.1017/9781139524100.023

will not consider it here. At the Hamiltonian level we have

$$H_{\text{dipole}} = -\frac{1}{2}\left(F_2\bar{f}(x)\sigma_{\mu\nu}f(x) + iF_3\bar{f}(x)\sigma_{\mu\nu}\gamma_5 f(x)\right)F^{\mu\nu}(x), \tag{17.9}$$

$$F^{\mu\nu}(x) = \partial_\mu A_\nu(x) - \partial_\nu A_\mu(x). \tag{17.10}$$

The formfactors F_2 and F_3 have negative energy dimension-1 and behave like $1/M$ with M being some energy scale. The operators in (17.9) have dimension-5. Their presence in the fundamental classical Lagrangian would spoil the renormalizability at the quantum field theory level. But they can be generated by quantum loop effects, and their absence in the classical Lagrangian guarantees that both a_f and d_f are finite and calculable in terms of fundamental parameters of the theory.

These considerations can be generalized to transition dipole moments relevant for $l_i \to l_j\gamma$ with $i \neq j$. One has then

$$\langle f_j(p')|J^{em}_\mu|f_i(p)\rangle = \bar{u}_j(p')\Gamma^{ij}_\mu u_i(p), \tag{17.11}$$

with

$$\Gamma^{ij}_\mu = (q^2 g_{\mu\nu} - q_\mu q_\nu)\gamma^\nu\left[F^{ij}_{E0}(q^2)\gamma_\mu + \gamma_5 F^{ij}_{M0}(q^2)\right] + i\sigma_{\mu\nu}q^\nu\left[F^{ij}_{M1}(q^2) + \gamma_5 F^{ij}_{E1}(q^2)\right], \tag{17.12}$$

where gauge invariance has been imposed.

The first structure is familiar from photon penguin diagram calculation and contributes to chirality conserving FCNC processes with $q^2 \neq 0$. It is then really a part of dimension-6 operator contribution to $\mu \to 3e$ and similar processes. On the other hand, F^{ij}_{M1} and F^{ij}_{E1} change chirality and are analogs of magnetic and electric dipole moments. The corresponding operators have dimension-5, and similar to a_f and d_f the formfactors F^{ij}_{M1} and F^{ij}_{E1} being generated at the quantum level are finite.

The decay rate is then given by

$$\Gamma(f_i \to f_j + \gamma) = \frac{1}{8\pi}\left(\frac{m^2_{f_i} - m^2_{f_j}}{m_{f_i}}\right)^3\left(|F^{ij}_{M1}|^2 + |F^{ij}_{E1}|^2\right) \tag{17.13}$$

with $f_i = \mu, \tau$ and $f_j = e, \mu$. This formula is, of course, valid also for $b \to s\gamma$ and $b \to d\gamma$ decays.

I hope the readers are now sufficiently motivated to make this step in our expedition, which at certain places is rather technical.

17.2 Lepton Flavor Violation

17.2.1 Preliminaries

The discovery of neutrino oscillations has shown that the individual lepton numbers are not conserved. However, no charged lepton flavor-violating decays have been observed to date.

Downloaded from https://www.cambridge.org/core. UNIVERSIDAD AUTONOMA METROPOLITANA, on 16 Nov 2026 at 21:17:32, subject to the Cambridge Core terms of use, available at https://www.cambridge.org/core/terms. https://doi.org/10.1017/9781139524100.023

In the SM enriched by light neutrino masses, lepton-flavor-violating decays $\ell_j \to \ell_i \gamma$ occur at unobservable small rates because the transition amplitudes are suppressed by a factor of $(m^2_{\nu_j} - m^2_{\nu_i})/M^2_W$. We will demonstrate this later.

On the other hand, in many extensions of the SM, like supersymmetric models, littlest Higgs model with T-parity (LHT), or models with vector-like leptons (VLLs) measurable in the coming years, branching ratios are predicted, in particular when the masses of involved new particles are in the LHC reach. However, it should be stressed that in principle LFV can even be sensitive to energy scales as high as 1000 TeV. We will return to this point in Chapter 19.

Additional interest in LFV arose in the last years due to indications of the violation of *lepton flavor universality* (LFU) in B decays, discussed in previous chapters. In some BSM models it implies measurable LFV branching ratios. We will discuss these intriguing implications only very briefly at the end of this section. For the time being we will assume LFU.

A very prominent role in the LFV studies is played by the radiative decays

$$\boxed{\mu \to e\gamma, \qquad \tau \to \mu\gamma, \qquad \tau \to e\gamma,} \tag{17.14}$$

which are analogs of $b \to s\gamma$ considered already by us. But the full picture of possible NP can only be obtained through a simultaneous study of the decays

$$\boxed{\mu^- \to e^-e^+e^-, \qquad \tau^- \to \mu^-\mu^+\mu^-, \qquad \tau^- \to e^-e^+e^-,} \tag{17.15}$$

$$\boxed{\tau^- \to e^-\mu^+\mu^-, \qquad \tau^- \to \mu^-e^+e^-, \qquad \tau^- \to \mu^-e^+\mu^-, \qquad \tau^- \to e^-\mu^+e^-,} \tag{17.16}$$

as well as of the $\mu - e$ conversion in nuclei. Also processes like $e^+\mu^- \to e^+e^-$ are of interest.

In this context let us mention already now how a clear-cut distinction between supersymmetric models, LHT model, and a model with a fourth sequential generation (SM4) is possible on the basis of all these decays. While it is not possible to distinguish the LHT model from the supersymmetric models on the basis of $\mu \to e\gamma$ alone, it has been pointed out in [1125] that such a distinction can be made by measuring any of the ratios $\mathcal{B}(\mu \to 3e)/\mathcal{B}(\mu \to e\gamma)$, $\mathcal{B}(\tau \to 3\mu)/\mathcal{B}(\tau \to \mu\gamma)$, etc. In supersymmetric models all these decays are governed by dipole operators so that these ratios are $O(\alpha)$ [1123, 1126–1131]. In the LHT model the LFV decays with three leptons in the final state are not governed by dipole operators but by Z-penguins and box diagrams, and the ratios in question turn out to be by almost an order of magnitude larger than in supersymmetric models. Other analyses of LFV in the LHT model can be found in [1132, 1133] and in the MSSM in [1123]. In the latter paper $(g-2)_e$ was used to probe lepton flavor-violating couplings that are correlated with $\tau \to e\gamma$. For a detailed analysis of the correlation between $\mu \to 3e$ and $(g-2)_\mu$, see [804]. A recent review of LFV including experimental prospects for coming years can be found in [1134].

Similarly, as pointed out in [1135], the pattern of the LFV branching ratios in the SM4 differs significantly from the one encountered in the MSSM, allowing to distinguish these

Downloaded from https://www.cambridge.org/core. UNIVERSIDAD AUTONOMA METROPOLITANA, on 16 Nov 2026 at 21:17:32, subject to the Cambridge Core terms of use, available at https://www.cambridge.org/core/terms. https://doi.org/10.1017/9781139524100.023

Table 17.1 Experimental upper limits on the branching ratios of the radiative lepton decays and experimental prospects.

Process	Experimental bound	Experimental prospects
$\mathcal{B}(\tau \to \mu\gamma)$	4.4×10^{-8} [1150]	4.4×10^{-9} [1151]
$\mathcal{B}(\tau \to e\gamma)$	3.3×10^{-8} [1150]	3.3×10^{-9}[1151]
$\mathcal{B}(\mu \to e\gamma)$	4.2×10^{-13} [1152]	4×10^{-14} [1139]
$\mathcal{B}(\mu \to e)$	$O(10^{-12})$ [1153]	10^{-17} [1154, 1155]

Table 17.2 Experimental upper limits on the branching ratios of the three body charged lepton decays and experimental prospects.

Process	Experimental bound	Experimental prospects
$\mathcal{B}(\mu^- \to e^-e^+e^-)$	1.0×10^{-12} [1156]	10^{-16} [1140]
$\mathcal{B}(\tau^- \to \mu^-\mu^+\mu^-)$	1.2×10^{-8} [150]	10^{-9} [1157]
$\mathcal{B}(\tau^- \to e^-e^+e^-)$	1.4×10^{-8} [150]	10^{-9} [1157]
$\mathcal{B}(\tau^- \to e^-\mu^+\mu^-)$	1.6×10^{-8} [150]	10^{-9} [1157]
$\mathcal{B}(\tau^- \to \mu^-e^+e^-)$	1.1×10^{-8} [150]	10^{-9} [1157]
$\mathcal{B}(\tau^- \to \mu^-e^+\mu^-)$	9.8×10^{-9} [150]	10^{-9} [1157]
$\mathcal{B}(\tau^- \to e^-\mu^+e^-)$	8.4×10^{-9} [150]	10^{-9} [1157]

two models with the help of LFV processes in a transparent manner. Also differences from the LHT model were identified. Even if fourth generation has been already ruled out, these studies demonstrate the power of a combined analysis of the decays in (17.14)–(17.16).

Of particular interest is the study of τ decays because as opposed to muon decays, we have at our disposal many more channels involving also pseudoscalar mesons in the final state. In fact hadronic τ decays offer powerful probes of NP in the LHC era [1136]. The physics reach and model-discriminating power of LFV tau decays is most efficiently analyzed above the electroweak scale using SMEFT and in the corresponding LEFT [1137]. For an earlier analysis, see [1138]. We will give the relevant formulas in Section 17.2.3.

A detailed analysis of LFV in various extensions of the SM is also motivated by the prospects (see Tables 17.1 and 17.2) for the measurements of LFV processes with much higher sensitivity than presently available. In particular, the MEG experiment at PSI is already testing $\mathcal{B}(\mu \to e\gamma)$ at the level of $O(10^{-13})$ putting severe constraints on the parameters of a number of models to be mentioned later. An upgrade for MEG is also already approved [1139] so that the sensitivity down to $4 \cdot 10^{-14}$ after three years of running is expected. There is also an approved proposal at PSI to do $\mu \to eee$ [1140]. The planned accuracy of SuperKEKB of $O(10^{-8})$ for $\tau \to \mu\gamma$ is also of great interest. This decay can also be studied by the LHCb experiment at CERN.

An improved upper bound on $\mu - e$ conversion in titanium will also be very important. In this context the dedicated J-PARC experiment PRISM/PRIME [1141] should reach

Downloaded from https://www.cambridge.org/core. UNIVERSIDAD AUTONOMA METROPOLITANA, on 16 Nov 2026 at 21:17:32, subject to the Cambridge Core terms of use, available at https://www.cambridge.org/core/terms. https://doi.org/10.1017/9781139524100.023

the sensitivity of $O(10^{-18})$, i. e., an improvement by six orders of magnitude relative to the present upper bound from SINDRUM-II at PSI [1142]. Similar comments apply to COMET at J-PARC [1143, 1144]. Mu2e collaboration will measure $\mu - e$ conversion on aluminium to $6 \cdot 10^{-17}$ at 90% CL around the year 2020 [1145], which is a factor of 10^4 better than SINDRUM-II. In [1146] the model discriminating power of a combined phenomenological analysis of $\mu \to e\gamma$ and $\mu \to e$ conversion on different nuclei targets is discussed. A nice summary of all these efforts is given in [1147].

For further detailed reviews of LFV, see [1117, 1148, 1149]. An experimenter's guide for charged LFV can be found in [1121]. In what follows we will first discuss these decays in the SM. Subsequently we will collect formulas for them that will be sufficiently general to allow motivated readers to perform analyses in specific NP scenarios. Having these formulas we will illustrate in Section 17.2.9 their application in the context of Z' models.

17.2.2 $\mu \to e\gamma$ in the SM

To calculate the rate for $\mu \to e\gamma$ in the SM, let us compare the diagrams contributing to the $B \to X_s\gamma$ and $\mu \to e\gamma$ decays. They are shown in Figures 17.1 and 17.2, respectively. In R_ξ gauges also the corresponding diagrams with Goldstone bosons contribute. The diagram with the photon coupled directly to the internal fermion line, present in $B \to X_s\gamma$, is absent in the case of $\mu \to e\gamma$ due to the vanishing neutrino charge.

In the case of the $B \to X_s\gamma$ decay the function $D_0'(x)$ resulting from the diagrams in Figure 17.1 can be decomposed as follows

$$D_0'(x) = \left[D_0'(x)\right]_{\text{Abelian}} + \left[D_0'(x)\right]_{\text{triple}}, \tag{17.17}$$

where the first term on the r.h.s. represents the sum of the first and the last diagram in Figure 17.1 and the second term represents the second diagram.

The inspection of an explicit calculation of the $b \to s\gamma$ transition in the 't Hooft–Feynman gauge gives

$$\left[D_0'(x)\right]^{b\to s\gamma}_{\text{Abelian}} = (2Q_d - Q_u)E_0'(x), \tag{17.18}$$

where $E_0'(x)$ is one of the one-loop master functions introduced in Chapter 6. Q_d and Q_u are the electric charges of external and internal fermions, respectively. Setting $Q_d = -1/3$ and $Q_u = 2/3$ in (17.18) and using (17.17), we find

$$\left[D_0'(x)\right]_{\text{triple}} = D_0'(x) + \frac{4}{3}E_0'(x). \tag{17.19}$$

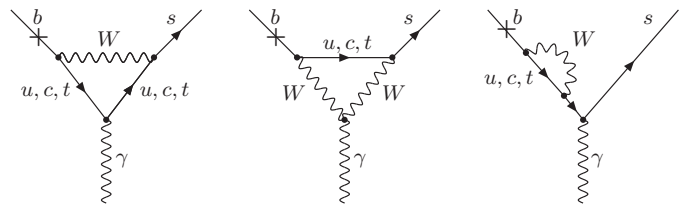


Figure 17.1 Diagrams contributing to $b \to s\gamma$ in the SM.

Downloaded from https://www.cambridge.org/core. UNIVERSIDAD AUTONOMA METROPOLITANA, on 16 Nov 2026 at 21:17:32, subject to the Cambridge Core terms of use, available at https://www.cambridge.org/core/terms. https://doi.org/10.1017/9781139524100.023

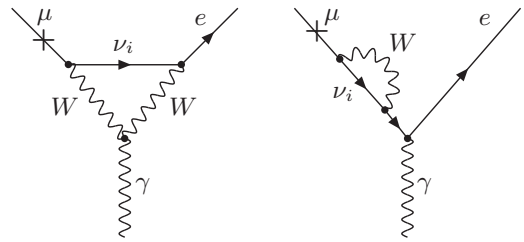


Figure 17.2 Diagrams contributing to $\mu \to e\gamma$ in the SM.

This contribution is independent of fermion electric charges and can be directly used in the $\mu \to e\gamma$ decay.

Turning now our attention to the latter decay, we find first from (17.18)

$$\left[D_0'(x)\right]^{\mu\to e\gamma}_{\text{Abelian}} = -2E_0'(x), \tag{17.20}$$

as $Q_u = Q_\nu = 0$ and $Q_d = Q_l = -1$ in this case. The final result for the relevant short-distance function in the case of $\mu \to e\gamma$ is then given by the sum of (17.19) and (17.20). Denoting this function by $H(x_\nu^i)$, we find

$$H(x_\nu^i) = D_0'(x_\nu^i) - \frac{2}{3}E_0'(x_\nu^i), \qquad x_\nu^i = \left(\frac{m_\nu^i}{M_W}\right)^2. \tag{17.21}$$

The generalization of the known SM result to arbitrary neutrino masses reads then

$$\mathcal{B}(\mu \to e\gamma)_{\text{SM}} = \frac{3\alpha}{2\pi}\left|\sum_i U_{ei}U_{\mu i}^* H(x_\nu^i)\right|^2, \tag{17.22}$$

with U_{ij} being the elements of the PMNS matrix.

Now, in the limit of small neutrino masses,

$$H(x_\nu^i) \longrightarrow \frac{x_\nu^i}{4} \qquad \text{as} \quad x_\nu^i \to 0, \tag{17.23}$$

and we confirm the known result

$$\mathcal{B}(\mu \to e\gamma)_{\text{SM}} = \frac{3\alpha}{32\pi}\left|\sum_i U_{ei}U_{\mu i}^* x_\nu^i\right|^2. \tag{17.24}$$

With the input in (2.112), we find

$$\mathcal{B}(\mu \to e\gamma)_{\text{SM}} \simeq 0.015\,\alpha\, s_{13}^2\left[\frac{\Delta m_{32}^2}{M_W^2}\right]^2 < 10^{-54}. \tag{17.25}$$

Certainly such branching ratios cannot be measured in this century.

Downloaded from https://www.cambridge.org/core. UNIVERSIDAD AUTONOMA METROPOLITANA, on 16 Nov 2026 at 21:17:32, subject to the Cambridge Core terms of use, available at https://www.cambridge.org/core/terms. https://doi.org/10.1017/9781139524100.023

17.2.3 LFV Decays and SMEFT

Preliminaries

Over several decades by now LFV decays and transitions have been studied in details in many extensions of the SM, in particular in supersymmetric models and models like LHT model, in which FCNCs are absent at tree-level. In such models LFV decays are governed by γ-penguin, Z-penguin, Higgs-penguin, and box diagrams with heavy new particles in the loop. Useful general expressions for branching ratios used in the MSSM have been derived in [1127, 1158] and used in the context of the LHT model in [1125]. The interested reader can look at these papers that in principle can be used in any extension of the SM. However, for models, like Z' models, LQ models, models with FCNC mediated by heavy scalars, where FCNC are entering already at tree-level, it is more efficient to use the SMEFT formulation. Yet, also in this case, as we will see soon, contributions of γ-penguins and their correlations with four-fermion operators have to be included.

For LFV in charged lepton decays such an analysis has been done in [795], and we will collect the main results of this paper here. Some of these expressions will also give us automatically the results for EDMs of leptons and also $(g-2)_{e,\mu}$ that will be discussed in two subsequent sections.

In Table 17.3 we collect the independent dimension-6 operators relevant for our discussion. It is a subset of the operators listed in Tables 14.1 and 14.2. These are all operators that can contribute to LFV processes in the charged lepton sector at the tree-level or at the 1-loop level. The operators that could give LFV effects only via the interference with the dimension-4 SM vertices containing the PMNS matrix are neglected because such effects are suppressed by the small neutrino masses. To simplify the notation, the flavor indices in the name of operators are suppressed in this table, but they will be exposed whenever it will be necessary. Here we just give one example that specifies the order of the flavor indices:

$$Q_{\ell\ell}^{jikl} = (\bar{\ell}_j \gamma_\mu \ell_i)(\bar{\ell}_k \gamma^\mu \ell_l) \tag{17.26}$$

with i, j, k, l running from 1 to 3. For instance, $i = 2 = \mu$, $i = 3 = \tau$, and $k = 1 = e$.

Table 17.3 Complete list of the dimension-6 operators (invariant under the SM gauge group) that contribute to the LFV observables under consideration at the tree- or at the one-loop level [795].

$\ell\ell\ell\ell$		$\ell\ell X\varphi$		$\ell\ell\varphi^2 D$ and $\ell\ell\varphi^3$	
$Q_{\ell\ell}$	$(\bar{\ell}_i\gamma_\mu\ell_j)(\bar{\ell}_k\gamma^\mu\ell_l)$	Q_{eW}	$(\bar{\ell}_o\sigma^{\mu\nu}e_j)\tau^I\varphi W^I_{\mu\nu}$	$Q^{(1)}_{\varphi\ell}$	$(\varphi^\dagger i\overleftrightarrow{\mathcal{D}_\mu}\varphi)(\bar{\ell}_i\gamma^\mu\ell_j)$
Q_{ee}	$(\bar{e}_i\gamma_\mu e_j)(\bar{e}_k\gamma^\mu e_l)$	Q_{eB}	$(\bar{\ell}_i\sigma^{\mu\nu}e_j)\varphi B_{\mu\nu}$	$Q^{(3)}_{\varphi\ell}$	$(\varphi^\dagger i\overleftrightarrow{\mathcal{D}^I_\mu}\varphi)(\bar{\ell}_i\tau^I\gamma^\mu\ell_j)$
$Q_{\ell e}$	$(\bar{\ell}_i\gamma_\mu\ell_j)(\bar{e}_k\gamma^\mu e_l)$			$Q_{\varphi e}$	$(\varphi^\dagger i\overleftrightarrow{\mathcal{D}_\mu}\varphi)(\bar{e}_i\gamma^\mu e_j)$
				$Q_{e\varphi 3}$	$(\varphi^\dagger\varphi)(\bar{\ell}_i e_j\varphi)$
		$\ell\ell qq$			
$Q^{(1)}_{\ell q}$	$(\bar{\ell}_i\gamma_\mu\ell_j)(\bar{q}_k\gamma^\mu q_l)$	$Q_{\ell d}$	$(\bar{\ell}_i\gamma_\mu\ell_j)(\bar{d}_k\gamma^\mu d_l)$	$Q_{\ell u}$	$(\bar{\ell}_i\gamma_\mu l_j)(\bar{u}_k\gamma^\mu u_l)$
$Q^{(3)}_{\ell q}$	$(\bar{\ell}_i\gamma_\mu\tau^I\ell_j)(\bar{q}_k\gamma^\mu\tau^I q_l)$	Q_{ed}	$(\bar{e}_i\gamma_\mu e_j)(\bar{d}_k\gamma^\mu d_l)$	Q_{eu}	$(\bar{e}_i\gamma_\mu e_j)(\bar{u}_k\gamma^\mu u_l)$
Q_{eq}	$(\bar{e}_i\gamma^\mu e_j)(\bar{q}_k\gamma_\mu q_l)$	$Q_{\ell edq}$	$(\bar{\ell}^a_i e_j)(\bar{d}_k q^a_l)$	$Q^{(1)}_{\ell equ}$	$(\bar{\ell}^a_i e_j)\varepsilon_{ab}(\bar{q}^b_k u_l)$
				$Q^{(3)}_{\ell equ}$	$(\bar{\ell}^a_i\sigma_{\mu\nu}e_a)\varepsilon_{ab}(\bar{q}^b_k\sigma^{\mu\nu}u_l)$

Downloaded from https://www.cambridge.org/core. UNIVERSIDAD AUTONOMA METROPOLITANA, on 16 Nov 2026 at 21:17:32, subject to the Cambridge Core terms of use, available at https://www.cambridge.org/core/terms. https://doi.org/10.1017/9781139524100.023

One could interchange, of course, j and i to have alphabetic ordering $ijkl$, but as the authors of [795] made this labeling, it is safer to keep it in this section. In case a reader will be lost in the indices, this formula should be useful as well as the discussion of the indices in section II of the latter paper.

In [795] the full one-loop predictions for the $\ell_i \to \ell_f \gamma$ decays and all tree-level contributions for $\ell_i \to \ell_j \bar{\ell}_l \ell_k$ decays in terms of the Wilson coefficients of the dimension-6 operators have been calculated. Motivated readers should have a look at this paper. In particular it has been found that the contributions of some of the operators in Table 17.3 can be neglected, and their Wilson coefficients will be absent in the final formulas for branching ratios.

17.2.4 General Formulas for $l_j^- \to l_i^- \gamma$ beyond the SM

We will first present the formulas in terms of WCs of more familiar operators, and subsequently we will relate them to the WCs of the SMEFT. We begin with the general form of the flavor-violating photon-lepton vertex that can be written in terms of vector, scalar, and dipole formfactors as follows

$$\boxed{V_{\ell\ell\gamma}^{fi\,\mu} = \frac{i}{\Lambda^2}\left[\gamma^\mu (F_{VL}^{fi} P_L + F_{VR}^{fi} P_R) + (F_{SL}^{fi} P_L + F_{SR}^{fi} P_R) q^\mu + (F_{TL}^{fi} i\sigma^{\mu\nu} P_L + F_{TR}^{fi} i\sigma^{\mu\nu} P_R) q_\nu\right].} \tag{17.27}$$

Once the formfactors entering this equation have been expressed in terms of WCs of the SMEFT operators, the branching ratios for the $\ell_i \to \ell_f \gamma$ decays (with $i > f$) at the 1-loop level up to the order $1/\Lambda^2$ can be directly given in terms of these WCs and used for any model. In addition, the obtained results are directly related to the EDMs and anomalous magnetic moments of leptons after setting $f = i$. We will use them in the next two sections.

Now, gauge-invariance requires that F_{VL} and F_{VR} must vanish for on-shell external particles. Moreover, the formfactors F_{SL} and F_{SR} do not contribute to the $\ell_i \to \ell_f \gamma$ decay amplitude. Therefore, finally the branching ratios can be expressed in terms of F_{TL}^{fi} and F_{TR}^{fi} only:

$$\boxed{\mathcal{B}\left(\ell_i \to \ell_f \gamma\right) = \frac{m_{\ell_i}^3}{16\pi\Lambda^4\,\Gamma_{\ell_i}}\left(\left|F_{TR}^{fi}\right|^2 + \left|F_{TL}^{fi}\right|^2\right).} \tag{17.28}$$

Here Γ_{ℓ_i} denotes the total decay width of the decaying lepton that was discussed in Chapter 3. Comparing with (17.13), evidently

$$\frac{F_{TR}}{\Lambda^2} = F_{M1} + F_{E1}, \qquad \frac{F_{TL}}{\Lambda^2} = F_{M1} - F_{E1}. \tag{17.29}$$

Now comes an important point. Among the operators in Table 17.3 only the operators Q_{eW} and Q_{eB} can contribute to $F_{TL,R}^{fi}$ at the tree-level. If their coefficients are comparable

Downloaded from https://www.cambridge.org/core. UNIVERSIDAD AUTONOMA METROPOLITANA, on 16 Nov 2026 at 21:17:32, subject to the Cambridge Core terms of use, available at https://www.cambridge.org/core/terms. https://doi.org/10.1017/9781139524100.023

to other Wilson coefficients of the dimension-6 operators, they dominate the effective photon-lepton vertex, with the formfactors simply given by ($v = 246\,\text{GeV}$):

$$\boxed{F_{TR}^{fi} = F_{TL}^{if*} = v\sqrt{2}\left(c_W C_{eB}^{fi} - s_W C_{eW}^{fi}\right) \equiv v\sqrt{2}C_{\gamma}^{fi}\,.} \tag{17.30}$$

Yet, as emphasized in [795], in a renormalizable theory of NP the operators Q_{eW} and Q_{eB} can only be generated at the loop-level while other operators, like the effective four-lepton couplings, can already be generated at the tree-level. In some extensions of the SM C_{eW} and C_{eB} may even not be generated at all [1159]. Thus, comparable (or even dominant) contributions to the flavor-violating lepton-lepton-photon vertex can come from other dimension-6 operators, which for consistency, as done in [795], should be included at the one-loop level.

The final expressions for the nonvanishing one-loop contributions are collected in Table 17.4, where the first order of expansions in $1/\Lambda^2$ and m_l has been kept. In this excellent approximation only the five Wilson coefficients $C_{\ell e}^{fjji}$, $C_{\ell equ}^{(3)fijj}$, $C_{\varphi\ell}^{(3)fi}$, $C_{\varphi e}^{fi}$, and $C_{\varphi\ell}^{(1)fi}$ contribute.

We note that the terms proportional to $C_{\ell equ}^{(3)}$ contain a divergence Δ. This divergence must be canceled by a counterterm to Q_{eW} and/or Q_{eB}. We refer to [795] for the discussion of this issue.

Table 17.4 One-loop contributions to formfactors F_{TL}^{fi} and F_{TR}^{fi} giving rise to $\ell_i \to \ell_f\gamma$ up to order $1/\Lambda^2$ [795].

Different contributions	Tensor formfactors
Z	$F_{TL}^{Z\,fi} = \dfrac{4e\left[\left(C_{\varphi\ell}^{(1)fi} + C_{\varphi\ell}^{(3)fi}\right) m_f (1+s_W^2) - C_{\varphi e}^{fi} m_i \left(\frac{3}{2} - s_W^2\right)\right]}{3(4\pi)^2}$
	$F_{TR}^{Z\,fi} = \dfrac{4e\left[\left(C_{\varphi\ell}^{(1)fi} + C_{\varphi l}^{(3)fi}\right) m_i (1+s_W^2) - C_{\varphi e}^{fi} m_f \left(\frac{3}{2} - s_W^2\right)\right]}{3(4\pi)^2}$
W	$F_{TL}^{W\,fi} = -\dfrac{10 e m_f C_{\varphi\ell}^{(3)fi}}{3(4\pi)^2}$
	$F_{TR}^{W\,fi} = -\dfrac{10 e m_i C_{\varphi\ell}^{(3)fi}}{3(4\pi)^2}$
Contact 4-fermion	$F_{TL}^{4f\,fi} = -\dfrac{16e}{3(4\pi)^2}\sum_{j=1}^{3} C_{\ell equ}^{(3)fijj\star} m_{u_j}\left(\Delta - \log\dfrac{m_{u_j}^2}{\mu^2}\right)$
	$F_{TR}^{4f\,fi} = -\dfrac{16e}{3(4\pi)^2}\sum_{j=1}^{3} C_{\ell equ}^{(3)fijj} m_{u_j}\left(\Delta - \log\dfrac{m_{u_j}^2}{\mu^2}\right)$
Contact 4-lepton	$F_{TL}^{4\ell\,fi} = \dfrac{2e}{(4\pi)^2}\sum_{j=1}^{3} C_{\ell e}^{fjji} m_j$
	$F_{TR}^{4\ell\,fi} = \dfrac{2e}{(4\pi)^2}\sum_{j=1}^{3} C_{\ell e}^{jifj} m_j$

Downloaded from https://www.cambridge.org/core. UNIVERSIDAD AUTONOMA METROPOLITANA, on 16 Nov 2026 at 21:17:32, subject to the Cambridge Core terms of use, available at https://www.cambridge.org/core/terms. https://doi.org/10.1017/9781139524100.023

17.2.5 General Formulas for $\ell_i \to \ell_j \bar{\ell}_l \ell_k$ beyond the SM

We will next present general formulas for the branching ratios of the seven decays listed in (17.15) and (17.16). The authors of [795] split the expressions for the $\ell_i \to \ell_j \bar{\ell}_l \ell_k$ decays into three groups, depending on the composition of the final state leptons:

(A) Three leptons of the same flavor: $\mu^- \to e^- e^+ e^-$, $\tau^- \to e^- e^+ e^-$, and $\tau^- \to \mu^- \mu^+ \mu^-$.
(B) Three distinguishable leptons: $\tau^- \to e^- \mu^+ \mu^-$ and $\tau^- \to \mu^- e^+ e^-$.
(C) Two leptons of the same flavor and charge and one with different flavor and opposite charge: $\tau^- \to \mu^- e^+ \mu^-$ and $\tau^- \to e^- \mu^+ e^-$.

To calculate the branching ratios the amplitude A for the decay $\ell_i \to \ell_j \bar{\ell}_l \ell_k$ is decomposed as

$$A = A_0 + A_\gamma, \tag{17.31}$$

where A_0 contains all operators for which one can neglect the momenta of the external leptons and A_γ is the photon contribution generated by Q_{eW} and Q_{eB} only. The amplitude A_0 can then be written as:

$$A_0 = \frac{1}{\Lambda^2} \sum_I C_I [\bar{u}(p_j) Q_I u(p_i)][\bar{u}(p_k) Q'_I v(p_l)], \tag{17.32}$$

where u and v are usual Dirac spinors, and the momenta assignments are indicated by the indices and are shown explicitly in figure 4 of [795].

For a given $(ji;kl)$ the various operators contributing to A_0 are

$$[Q_{VXY}]^{ji}_{kl} = (\bar{\psi}_j \gamma^\mu P_X \psi_i)(\bar{\psi}_k \gamma_\mu P_Y \psi_l), \qquad [Q_{SXY}]^{ji}_{kl} = (\bar{\psi}_j P_X \psi_i)(\bar{\psi}_k P_Y \psi_l) \tag{17.33}$$

$$[Q_{TXX}]^{ji}_{kl} = (\bar{\psi}_j \sigma^{\mu\nu} P_X \psi_i)(\bar{\psi}_k \sigma_{\mu\nu} P_X \psi_l), \tag{17.34}$$

with X, Y standing for the chiralities L and R. The corresponding effective Hamiltonian is then simply given as

$$[\Delta \mathcal{H}_{\text{eff}}]^{ji}_{kl} = -\frac{1}{\Lambda^2} \sum_{X,Y} \left([C_{VXY}]^{ji}_{kl} [Q_{VXY}]^{ji}_{kl} + [C_{SXY}]^{ji}_{kl} [Q_{SXY}]^{ji}_{kl} + [C_{TXX}]^{ji}_{kl} [Q_{TXX}]^{ji}_{kl} \right), \tag{17.35}$$

so that in the branching ratios that follow we will encounter the coefficients C_{VLL}, C_{VLR}, C_{SLL}, C_{SLR}, C_{TLL}, and those with L and R interchanged.

The complication arises when two identical leptons are present in the final state because then one has to include crossed diagrams in which a different ordering of spinors appears. Using Fierz transformations collected in Appendix A.3, one can always bring the sum of these diagrams into the form in (17.32) but the presence of two diagrams has an effect on the Wilson coefficients of the relevant operators. In addition, when calculating branching ratios a factor 1/2 has to be included.

Downloaded from https://www.cambridge.org/core. UNIVERSIDAD AUTONOMA METROPOLITANA, on 16 Nov 2026 at 21:17:32, subject to the Cambridge Core terms of use, available at https://www.cambridge.org/core/terms. https://doi.org/10.1017/9781139524100.023

The contributions from photon exchange for various types of decays (A), (B), (C) read (retaining only $1/\Lambda^2$ terms) [795] ($p_{ij} = p_i - p_j$)

$$A_\gamma^{(A)} = \frac{ev}{\Lambda^2}\left(\frac{1}{p_{ij}^2}[\bar{u}(p_j)i\sigma^{\mu\nu}(C_{\gamma L}P_L + C_{\gamma R}P_R)(p_{ij})_\nu u(p_i)][\bar{u}(p_k)\gamma_\mu v(p_l)] - (p_j \leftrightarrow p_k)\right),$$
$$A_\gamma^{(B)} = \frac{ev}{\Lambda^2}\frac{1}{p_{ij}^2}[\bar{u}(p_j)i\sigma^{\mu\nu}(C_{\gamma L}P_L + C_{\gamma R}P_R)(p_{ij})_\nu u(p_i)][\bar{u}(p_k)\gamma_\mu v(p_l)],$$
$$A_\gamma^{(C)} = 0. \tag{17.36}$$

They bring in two additional coefficients $C_{\gamma L}$ and $C_{\gamma R}$.

The general expression for the spin averaged square matrix element $\mathcal{M} = \frac{1}{2}\sum_{pol}|A|^2$ can be significantly simplified by using the hierarchy of the charged lepton masses: $m_i \equiv M \gg m_j, m_k, m_l$. That is, $M = m_\mu$ or $M = m_\tau$. One finds then [795]

$$\begin{aligned}\mathcal{B}(\ell_i \to \ell_j\bar{\ell}_l\ell_k) = \frac{N_c M^5}{6144\pi^3\Lambda^4\Gamma_{\ell_i}}\Big(&4\left(|C_{VLL}|^2 + |C_{VRR}|^2 + |C_{VLR}|^2 + |C_{VRL}|^2\right)\\ &+ |C_{SLL}|^2 + |C_{SRR}|^2 + |C_{SLR}|^2 + |C_{SRL}|^2\\ &+ 48\left(|C_{TLL}|^2 + |C_{TRR}|^2\right) + X_\gamma\Big),\end{aligned} \tag{17.37}$$

where $N_c = 1/2$ if two of the final state leptons are identical, $N_c = 1$ in all other cases, and Γ_{ℓ_i} is the total decay width of the initial lepton. The photon penguin contribution is a bit more complicated and reads

$$\begin{aligned}X_\gamma^{(A)} &= -\frac{16ev}{M}\mathrm{Re}\left[\left(2C_{VLL} + C_{VLR} - \frac{1}{2}C_{SLR}\right)C_{\gamma R}^\star + \left(2C_{VRR} + C_{VRL} - \frac{1}{2}C_{SRL}\right)C_{\gamma L}^\star\right]\\ &\quad + \frac{64e^2v^2}{M^2}\left(\log\frac{M^2}{m^2} - \frac{11}{4}\right)(|C_{\gamma L}|^2 + |C_{\gamma R}|^2),\\ X_\gamma^{(B)} &= -\frac{16ev}{M}\mathrm{Re}\left[(C_{VLL} + C_{VLR})\,C_{\gamma R}^\star + (C_{VRR} + C_{VRL})\,C_{\gamma L}^\star\right]\\ &\quad + \frac{32e^2v^2}{M^2}\left(\log\frac{M^2}{m^2} - 3\right)(|C_{\gamma L}|^2 + |C_{\gamma R}|^2),\\ X_\gamma^{(C)} &= 0.\end{aligned} \tag{17.38}$$

Having these general formulas at hand, the next step is to express the coefficients C_I appearing in these formulas in terms of the WCs of the SMEFT operators. This has been done in [795], and we will now collect their results.

Downloaded from https://www.cambridge.org/core. UNIVERSIDAD AUTONOMA METROPOLITANA, on 16 Nov 2026 at 21:17:32, subject to the Cambridge Core terms of use, available at https://www.cambridge.org/core/terms. https://doi.org/10.1017/9781139524100.023

17.2.6 $\mu^- \to e^-e^+e^-, \tau^- \to \mu^-\mu^+\mu^-, \tau^- \to e^-e^+e^-$ in the SMFT

$$
\begin{aligned}
C_{VLL} &= 2\left((2s_W^2-1)\left(C_{\varphi\ell}^{(1)ji}+C_{\varphi\ell}^{(3)ji}\right)+C_{\ell\ell}^{jiij}\right),\\
C_{VRR} &= 2\left(2s_W^2 C_{\varphi e}^{ji}+C_{ee}^{jiij}\right),\\
C_{VLR} &= -\frac{1}{2}C_{SRL} = 2s_W^2\left(C_{\varphi\ell}^{(1)ji}+C_{\varphi\ell}^{(3)ji}\right)+C_{\ell e}^{jiij},\\
C_{VRL} &= -\frac{1}{2}C_{SLR} = (2s_W^2-1)C_{\varphi e}^{ji}+C_{\ell e}^{jiji},\\
C_{SLL} &= C_{SRR} = C_{TLL} = C_{TRR} = 0,\\
C_{\gamma L} &= \sqrt{2}C_\gamma^{ij*},\\
C_{\gamma R} &= \sqrt{2}C_\gamma^{ji}, \qquad \text{with } C_\gamma^{ji} \text{ in (17.30).}
\end{aligned}
\tag{17.39}
$$

17.2.7 $\tau^- \to e^-\mu^+\mu^-$ and $\tau^- \to \mu^-e^+e^-$ in the SMFT

Before giving the results for these decays let us make a few comments to distinguish them from the previous ones. They do not have identical leptons in the final state and have two types of contributions. First of all, they proceed as in $\tau^- \to \mu^-\mu^+\mu^-$ and $\tau^- \to e^-e^+e^-$ through $\Delta L = 1$ tree, penguin, and box diagrams. As there are no identical particles in the final state, the effective Hamiltonians for these contributions can be directly obtained from the decay $B \to X_s\ell^+\ell^-$, and this is a good exercise for any reader that reached so far. In case of difficulties an explicit derivation of the effective Hamiltonian for $\tau^- \to \mu^-e^+e^-$ is presented in the context of the LHT model in [1125]. The generalization to $\tau^- \to e^-\mu^+\mu^-$ is automatic.

But these decays can also receive $\Delta L = 2$ contributions and also in this case an explicit derivation of the branching ratio in the context of the LHT model can be found in [1125]. Which of the contributions dominates the branching ratios depends to some extent on the pattern of flavor-violating couplings. But quite generally $\Delta L = 1$ contributions dominate.

For these decays the WCs of the most familiar operators are related to the SMEFT ones as follows [795]

$$
\begin{aligned}
C_{VLL} &= (2s_W^2-1)\left(C_{\varphi\ell}^{(1)ji}+C_{\varphi l}^{(3)ji}\right)+C_{\ell\ell}^{jikk},\\
C_{VRR} &= 2s_W^2 C_{\varphi e}^{ji}+C_{ee}^{jikk},\\
C_{VLR} &= 2s_W^2\left(C_{\varphi\ell}^{(1)ji}+C_{\varphi\ell}^{(3)ji}\right)+C_{\ell e}^{jikk},\\
C_{VRL} &= (2s_W^2-1)C_{\varphi e}^{ji}+C_{\ell e}^{jkki},\\
C_{SLR} &= -2C_{\ell e}^{jkki},\\
C_{SRL} &= -2C_{\ell e}^{jikk},\\
C_{SLL} &= C_{SRR} = C_{TLL} = C_{TRR} = 0,\\
C_{\gamma L} &= \sqrt{2}C_\gamma^{ij*},\\
C_{\gamma R} &= \sqrt{2}C_\gamma^{ji}.
\end{aligned}
\tag{17.40}
$$

Downloaded from https://www.cambridge.org/core. UNIVERSIDAD AUTONOMA METROPOLITANA, on 16 Nov 2026 at 21:17:32, subject to the Cambridge Core terms of use, available at https://www.cambridge.org/core/terms. https://doi.org/10.1017/9781139524100.023

17.2.8 $\tau^- \to \mu^- e^+ \mu^-$ and $\tau^- \to e^- \mu^+ e^-$ in the SMFT

In these decays either there are two muons or two electrons in the final state with the third lepton being e^+ and μ^+, respectively. These decays can proceed at tree-level. In models in which FCNC appear first at one-loop level, like the LHT model, they are dominated by box-diagrams as Z-penguins and γ-penguins cannot contribute. As these two decays are of $\Delta L = 2$ type, they are generally strongly suppressed. The relevant effective Hamiltonian can be obtained from $\Delta F = 2$ processes in the quark sector by properly changing flavors and taking into account that two identical particles are present in the final state. Interested readers can find the construction of the effective Hamiltonian and the calculation of branching ratios for the case of the LHT model in [1125]. The resulting branching ratio is very strongly suppressed. Here we just quote the result from [795]

$$\begin{aligned} C_{VLL} &= 2C_{\ell\ell}^{kikj}, \\ C_{VRR} &= 2C_{ee}^{kikj}, \\ C_{VLR} &= -\frac{1}{2}C_{SRL} = C_{\ell e}^{kikj}, \\ C_{VRL} &= -\frac{1}{2}C_{SLR} = C_{\ell e}^{kjki}, \\ C_{SLL} &= C_{SRR} = C_{TLL} = C_{TRR} = 0, \\ C_{\gamma L} &= C_{\gamma R} = 0. \end{aligned} \tag{17.41}$$

17.2.9 Three-Body Decays in Z' Models

Calculating in Z' models directly tree diagrams for the three classes (A) – (C) just discussed, one finds for each of them the Wilson coefficient

$$[C_{VXY}]_{kl}^{ji} = -\frac{\Delta_X^{ji}(Z')\Delta_Y^{kl}(Z')}{M_{Z'}^2}, \tag{17.42}$$

where the minus sign is the consequence of the definition of WCs by the Lagrangian and not the Hamiltonian.

In calculating the branching ratios for the three classes of decays just discussed, we note that always $i \neq j$, but dependently on the class considered $k = l$ and/or $k \neq l$.

Class A

As defined earlier, these are decays with $k = l$ only. The presence of two identical leptons in the final state requires the introduction of a factor 1/2 at the level of the branching ratio. Moreover, always two diagrams, differing by the interchange of identical leptons, contribute. They interfere with each other for VLL and VRR cases but not for VLR and VRL. We find then ($\Gamma_\tau = 1/\tau_\tau$)

Downloaded from https://www.cambridge.org/core. UNIVERSIDAD AUTONOMA METROPOLITANA, on 16 Nov 2026 at 21:17:32, subject to the Cambridge Core terms of use, available at https://www.cambridge.org/core/terms. https://doi.org/10.1017/9781139524100.023

$$\boxed{\mathcal{B}(\tau^- \to \mu^-\mu^+\mu^-) = \frac{m_\tau^5}{1536\pi^3\Gamma_\tau}\left[2|C_{VLL}|^2 + 2|C_{VRR}|^2 + |C_{VLR}|^2 + |C_{VRL}|^2\right]_{\mu\mu}^{\mu\tau},} \tag{17.43}$$

with analogous expressions for $\mu^- \to e^-e^+e^-$ and $\tau^- \to e^-e^+e^-$. Γ_τ is the total τ decay width.

Class B

Here both $k = l$ and $k \neq l$ are possible, but there are no identical leptons in the final state so that the branching ratio can easily be obtained from the formula for μ or τ decay in the limit of vanishing final lepton masses. We find then for the $\Delta L = 1$ contribution

$$\boxed{\mathcal{B}(\tau^- \to \mu^-e^+e^-) = \frac{m_\tau^5}{1536\pi^3\Gamma_\tau}\left[|C_{VLL}|^2 + |C_{VRR}|^2 + |C_{VLR}|^2 + |C_{VRL}|^2\right]_{ee}^{\mu\tau},} \tag{17.44}$$

with an analogous expression for $\tau^- \to e^-\mu^+\mu^-$. To obtain $\Delta L = 2$ contribution μ^- and e^- should be interchanged.

Class C

Here we only have $k \neq l$ but two identical leptons in the final state. We find similar to Class A

$$\boxed{\mathcal{B}(\tau^- \to \mu^-e^+\mu^-) = \frac{m_\tau^5}{1536\pi^3\Gamma_\tau}\left[2|C_{VLL}|^2 + 2|C_{VRR}|^2 + |C_{VLR}|^2 + |C_{VRL}|^2\right]_{\mu e}^{\mu\tau},} \tag{17.45}$$

with an analogous expression for $\tau^- \to e^-\mu^+e^-$.

These formulas agree with the ones present in FLAVIO [813] and the first two with [1128], where the result for class C has not been given. They can also be derived from (17.37), but the route to them is a bit different, which explains the additional factors in the formulas (17.43) and (17.45) relative to (17.37).

The reason for this difference is that the authors in [795] look first at all diagrams and making Fierz transformations in the case of Classes A and C, they bring the amplitude into the form (17.32). In the VLL and VRR cases the Fierz transformation for fields does not change the Dirac structure of the operator so that the coefficient VLL or VRR in that paper gets a factor of two. Squaring it to obtain the branching ratio and multiplying by 1/2, because of identical fermions, one reproduces our factors of 2 in (17.43) and (17.45).

More interesting is the case VLR as the Fierz transformation results in the operator SRL multiplied by -2. But as seen in (17.37) the contribution of this operator to the branching ratio misses the factor 4 present in VLR contribution. This is compensated by $(-2)^2$ when squaring the Wilson coefficient in the evaluation of the branching ratio. At the end these two contributions are equal to each other, and multiplying their sum by 1/2 gives the last two terms in (17.43) and (17.45).

Downloaded from https://www.cambridge.org/core. UNIVERSIDAD AUTONOMA METROPOLITANA, on 16 Nov 2026 at 21:17:32, subject to the Cambridge Core terms of use, available at https://www.cambridge.org/core/terms. https://doi.org/10.1017/9781139524100.023

Table 17.5 Experimental upper limits (95 % CL) on the lepton flavor-violating Z^0 decay rates.

Process	Experimental bound
$\mathcal{B}\left[Z^0 \to \mu^\pm e^\mp\right]$	7.5×10^{-7} [35]
$\mathcal{B}\left[Z^0 \to \tau^\pm e^\mp\right]$	9.8×10^{-6} [35]
$\mathcal{B}\left[Z^0 \to \tau^\pm \mu^\mp\right]$	1.2×10^{-5} [35]

17.2.10 Lepton Flavor-Violating *Z* Decays

In [795] also lepton flavor-violating decays of the SM Z boson $Z \to \ell_f^- \ell_i^+$ have been calculated, and we list the results here. They will constitute an important constraint on NP couplings when the data improve. One finds

$$\boxed{\mathcal{B}\left(Z \to \ell_f^\pm \ell_i^\mp\right) = \frac{M_Z}{24\pi\Gamma_Z}\left[\frac{M_Z^2}{2}\left(\left|C_{fi}^{ZR}\right|^2 + \left|C_{fi}^{ZL}\right|^2\right) + \left|\Gamma_{fi}^{ZL}\right|^2 + \left|\Gamma_{fi}^{ZR}\right|^2\right],} \tag{17.46}$$

where $\Gamma_Z \approx 2.495$ GeV is the total decay width of the Z boson. Including all tree-level contributions, the authors of [795] find

$$\Gamma_{fi}^{ZL} = \frac{e}{2s_W c_W}\left(\frac{v^2}{\Lambda^2}\left(C_{\varphi l}^{(1)fi} + C_{\varphi l}^{(3)fi}\right) + \left(1 - 2s_W^2\right)\delta_{fi}\right), \tag{17.47}$$

$$\Gamma_{fi}^{ZR} = \frac{e}{2s_W c_W}\left(\frac{v^2}{\Lambda^2} C_{\varphi e}^{fi} - 2s_W^2 \delta_{fi}\right), \tag{17.48}$$

$$C_{fi}^{ZR} = C_{if}^{ZL\star} = -\frac{v}{\sqrt{2}\Lambda^2} C_Z^{fi}, \tag{17.49}$$

where C_Z^{fi} is defined as

$$C_Z^{fi} = \left(s_W C_{eB}^{fi} + c_W C_{eW}^{fi}\right). \tag{17.50}$$

The experimental bounds on these decays are given in Table 17.5. It should be kept in mind that that theoretical prediction in (17.46) is for the decay $Z \to \ell_f^- \ell_i^+$ or $Z \to \ell_f^+ \ell_i^-$ while the experimental values are for the sum $Z \to \ell_f^- \ell_i^+ + \ell_i^- \ell_f^+$. Therefore, (17.46) must be multiplied by a factor of 2 to compare it with the experimental values.

Z' contributions to $Z \to \ell_f^\pm \ell_i^\mp$ decays are generated by $Z - Z'$ mixing and given by

$$\mathcal{B}(Z \to \ell_i^+ \ell_j^-) = \sin^2\xi \frac{M_Z}{24\pi\Gamma_Z}\left[|\Delta_L^{ij}(Z')|^2 + |\Delta_R^{ij}(Z')|^2\right]. \tag{17.51}$$

17.2.11 $\mu - e$ Conversion in Nuclei

We give next the formulas for the μ-e conversion in nuclei, that is

$$\mu + (A, Z) \to e + (A, Z), \tag{17.52}$$

where Z and A denote the proton and atomic numbers in a nucleus, respectively.

Downloaded from https://www.cambridge.org/core. UNIVERSIDAD AUTONOMA METROPOLITANA, on 16 Nov 2026 at 21:17:32, subject to the Cambridge Core terms of use, available at https://www.cambridge.org/core/terms. https://doi.org/10.1017/9781139524100.023

Here we follow [1158], where general formulas can be found. The effective Lagrangian relevant to this process at the quark level as given in that paper includes photon-penguin, Z-penguin, and box-type diagrams. But the part involving the Z-penguin and box-diagrams can be combined and rewritten just in terms four fermion operators so that it can be used for operators contributing also at tree-level. Writing then the effective Lagrangian as

$$\begin{aligned}\mathcal{L}_{eff} = -\frac{e^2}{q^2}\bar{e}\left[q^2\gamma_\alpha(A_1^L P_L + A_1^R P_R) + m_\mu i\sigma_{\alpha\beta}q^\beta(A_2^L P_L + A_2^R P_R)\right]\mu \\ \times \sum_{q=u,d} Q_{em}^q \bar{q}\gamma^\alpha q \\ + e^2 \sum_{q=u,d} \bar{q}\gamma_\alpha q\ \bar{e}\gamma^\alpha(D_q^L P_L + D_q^R P_R)\mu,\end{aligned} \tag{17.53}$$

where the first term comes from the photon penguin-type diagrams and the second from any four-fermion operator having the appropriate flavors. The coefficient Q_{em}^q denotes the electric charge of the quark q.

Comparing this effective Lagrangian with the one in [1158] and using their results we find the rate

$$\begin{aligned}\Gamma(\mu \to e) = 4\alpha^5 \frac{Z_{eff}^4}{Z}|F(q)|^2\, m_\mu^5 \left[|Z(A_1^L - A_2^R) - (2Z+N)D_u^L - (Z+2N)D_d^L|^2\right. \\ \left. +|Z(A_1^R - A_2^L) - (2Z+N)D_u^R - (Z+2N)D_d^R|^2\right],\end{aligned} \tag{17.54}$$

where Z and N denote the proton and neutron numbers in a nucleus, respectively. Z_{eff} is an effective parameter and $F(q^2)$ the nuclear formfactor. In $^{48}_{22}$Ti, one finds $Z_{eff} = 17.6$ and $F(q^2 \simeq -m_\mu^2) \simeq 0.54$ [1161].

Renormalization group analysis below the EW scale including correlations with $\mu \to e\gamma$ and $\mu \to 3e$ has been presented in [796].

17.2.12 $K_{L,S} \to \mu e$ and $K_{L,S} \to \pi^0 \mu e$

In the SM the decay $K_L \to \mu e$ is forbidden at the tree-level but can proceed through box diagrams in the case of nondegenerate neutrino masses. Similar to $\mu \to e\gamma$ it is too small to be measured.

It is also known from the studies of the Pati–Salam (PS) model [968, 1162] where it proceeds through a tree-level LQ exchange in the t-channel. The stringent upper bound on its branching ratio[1163],

$$\mathcal{B}(K_L \to \mu e) = \mathcal{B}(K_L \to \mu^+ e^-) + \mathcal{B}(K_L \to \mu^- e^+) < 4.7 \cdot 10^{-12}, \tag{17.55}$$

Downloaded from https://www.cambridge.org/core. UNIVERSIDAD AUTONOMA METROPOLITANA, on 16 Nov 2026 at 21:17:32, subject to the Cambridge Core terms of use, available at https://www.cambridge.org/core/terms. https://doi.org/10.1017/9781139524100.023

implies the mass of the leptoquark gauge boson to be above 10^3 TeV [1164]. By increasing the weak gauge group of the PS model in the context of the so-called Petite Unification [1164, 1165] and placing ordinary fermions in multiplets with heavy new fermions, and not with the ordinary SM fermions as in the PS model, it is possible to avoid tree-level contributions to $K_L \to \mu e$ so that the process is dominated by the box diagrams with new heavy-gauge bosons, heavy quarks, and heavy leptons exchanged. The relevant masses of these particles can then be decreased to $O(1\,\text{TeV})$ without violating the bound in (17.55).

More recently the studies of this decay and related decays like $K_S^0 \to \pi^0 \mu^+ e^-$ intensified in view of hints for LFUV in B decays [995, 1160, 1166, 1167]. As discussed extensively in the last paper in this list and in section 4 of [305], both NA62 and LHCb Upgrade II phase will allow to study this issue. In this context one should also mention the analysis in [1168], where the impact of LFUV effects on $K \to \pi\nu\bar{\nu}$ has been investigated.

17.2.13 Lepton Flavor-Violating *B* Decays

These decays are useful for tests of the violation of flavor universality. We give here only references to papers in which these decays have been analyzed. These papers contain useful formulas. In [779] these decays and also those with $K^{(*)}\ell^+\ell'^-$ in the final state have been studied. In [1125] these decays have been studied in the LHT model. Specific application to Z' models is given in [1160] and in 2HDM III model in [995]. The last two papers discuss simultaneously charged lepton flavor violation. In particular in [1160] LFV B decays in generic Z' models have been discussed. Constraints from LFV in charged lepton decays have been considered. It has been found that $\tau \to 3\mu$ and $\tau \to \mu\nu\bar{\nu}$ but also $B_s^0 - \bar{B}_s^0$ mixing provide very strong constraints. Finally, the recent improved bounds on $B_d^0 \to \mu^\pm\tau^\mp$ $B_s^0 \to \mu^\pm\tau^\mp$ and $B^+ \to K^+\mu^\pm e^\mp$ from the LHCb put some pressure on models explaining B-physics anomalies.

The experimental bounds on the sums $\ell^\pm\ell'^\mp = \ell^-\ell'^+ + \ell^+\ell'^-$ are given in Table 17.6.

Table 17.6 Current limits on branching ratios for LFV decay channels.

Channel	Branching ratio	Reference
$K^+ \to \pi^+\mu^+e^-$	$\le 1.3 \times 10^{-11}$	E865, E777 [1169]
$K^+ \to \pi^+\mu^-e^+$	$\le 5.2 \times 10^{-10}$	E865 [1170]
$K_L \to \pi^0\mu^\pm e^\mp$	$\le 7.6 \times 10^{-11}$	KTeV [1171]
$K_L \to \mu^\pm e^\mp$	$\le 4.7 \times 10^{-12}$	E871 [1163]
$B_d^0 \to \mu^\pm e^\mp$	$\le 1.3 \times 10^{-9}$	LHCb [1172]
$B_s^0 \to \mu^\pm e^\mp$	$\le 6.3 \times 10^{-9}$	LHCb [1172]
$B_d^0 \to \mu^\pm \tau^\mp$	$\le 1.2 \times 10^{-5}$	LHCb [1173]
$B_s^0 \to \mu^\pm \tau^\mp$	$\le 3.4 \times 10^{-5}$	LHCb [1173]
$B^+ \to K^+\tau^\pm\mu^\mp$	$\le 4.8 \times 10^{-5}$	[35]
$B^+ \to K^+\mu^\pm e^\mp$	$\le 7.1 \times 10^{-9}$	LHCb
$B \to K^*\mu^\pm e^\mp$	$\le 1.4 \times 10^{-6}$	[35]

Downloaded from https://www.cambridge.org/core. UNIVERSIDAD AUTONOMA METROPOLITANA, on 16 Nov 2026 at 21:17:32, subject to the Cambridge Core terms of use, available at https://www.cambridge.org/core/terms. https://doi.org/10.1017/9781139524100.023

17.3 Electric Dipole Moments (EDMs)

17.3.1 Preliminaries

Even though the experimental sensitivities have improved a lot no EDM of a fundamental particle has been observed so far, and we have only upper bounds on them to our disposal that we collected in Table 17.7. Nevertheless, EDM experiments have already put strong limits on NP models. A permanent EDM of a fundamental particle violates both T and P, and thus – assuming CPT symmetry – is another way to measure CP violation. In the SM the individual quark EDMs vanish at two-loop order [1174, 1175] so that the only CP-violating phase of the CKM matrix enters quark EDMs first at three loop, which results in negligibly small SM EDMs. EDMs of leptons are in the SM even stronger suppressed than quark EDMs and enter first at four-loop level [1176]. Consequently EDMs are excellent probes of new CP-violating phases of NP models, especially flavor-blind phases, and of strong CP violation related to the so-called θ parameter.

The fact that EDMs are so strongly suppressed in the SM makes them very special compared to most observables considered in this book. A measurement of a nonvanishing EDM of any particle including nucleons, nuclei, atoms, and molecules will be a clear signal of NP similar to lepton flavor-violating processes. But whereas the latter are in most cases theoretically clean, the case of EDMs is very different. In addition to the short-distance dynamics present in the Wilson coefficients of contributing operators, not only hadronic physics as in other sections, but often also nuclear physics including nuclear many-body calculations and atomic physics is responsible for the final value of a given EDM. Therefore the identification of NP responsible through a measurement of a nonvanishing EDM is much more challenging than is the case of remaining observables considered in this book. Similar the determination of NP scale responsible is harder, but as in the case of rare K and B decays and LFV, EDMs can in principle probe short-distance scales far beyond the reach of the LHC.

As we will see later there are different sources for EDMs. For hadronic EDMs there is the θ term of QCD, which is very much constrained due to the nonobservation of permanent EDMs of the mercury atom (^{199}Hg) and neutron. Apart from the θ term, the SM CKM induced EDMs would be far smaller in magnitude than the next-generation EDM sensitivities. Consequently, one does not need the same kind of refined

Table 17.7 Current experimental upper bounds (at 90% C.L.) on electric dipole moments.

EDM	$\lvert d_e \rvert$	$\lvert d_\mu \rvert$	d_τ
Bound (e cm)	1.1×10^{-29} [1177]	1.5×10^{-19} [1178]	3.4×10^{-17} [1179]
EDM	$\lvert d_n \rvert$	$\lvert d_{Hg} \rvert$	d_{Tl}
Bound (e cm)	3.0×10^{-26} [1180]	6.3×10^{-30} [1181]	9.4×10^{-25} [1182]
EDM	$\lvert d_{Xe} \rvert$	$\lvert d_{Ra} \rvert$	
Bound (e cm)	1.4×10^{-27} [1183, 1334]	1.2×10^{-23} [1184, 1185]	

Downloaded from https://www.cambridge.org/core. UNIVERSIDAD AUTONOMA METROPOLITANA, on 16 Nov 2026 at 21:17:32, subject to the Cambridge Core terms of use, available at https://www.cambridge.org/core/terms. https://doi.org/10.1017/9781139524100.023

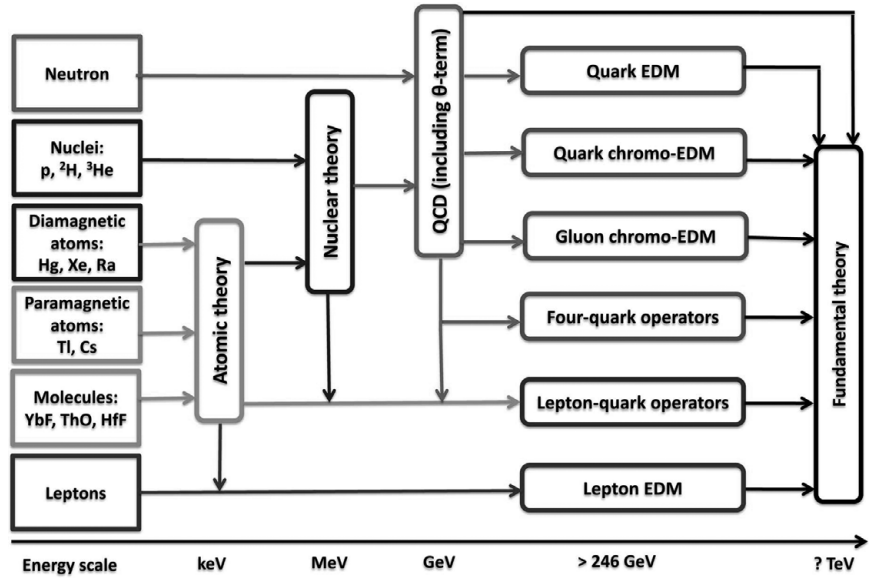


Figure 17.3 EDMs landscape. From Jordy De Vries.

hadronic structure computations as one often needs in flavor physics to interpret the EDM results in terms of NP. That being said, the hadronic matrix element problem remains a considerable challenge. At dimension-6 one encounters several different operators for the first generation fermions that could give rise to EDMs: pure gauge operators $\tilde{G}GG$, four-fermion operators (semileptonic and nonleptonic), gauge-Higgs operators $\varphi^\dagger\varphi\tilde{G}G$ and gauge-Higgs-fermion operators $(\bar{Q}T^A q_R)\varphi G$. We will be more specific about them later.

In experiments one often deals with composite systems, and thus nuclear physics is important in determining the EDMs of neutral atoms. Nuclear structure can also provide an amplifier of atomic EDMs. In heavier neutral systems there is the shielding of the EDMs of constituents of one charge by those of the other (e.g., protons and electrons). The transmission of CP violation through a nucleus into an atom must overcome this shielding. Its effectiveness in doing so is expressed by a nuclear Schiff moment. In nuclei with asymmetric shapes Schiff moments can be enhanced by two or even three orders of magnitude. For example, an octupole deformed nuclei such as ^{225}Ra give enhanced nuclear Schiff moments and, thus, enhanced atomic EDMs in a diamagnetic system.

Because of many sources of EDMs and significant theoretical uncertainties, it is a challenge to present this topic in a transparent manner. But this topic is very important, and it is mandatory to include it in this book and face this challenge. As seen in Figure 17.3, the connection between the fundamental theory and EDMs in measurable systems is rather involved. Our main goal for next pages is to present this problematic in explicit terms and to illuminate the connections between various elements of theoretical calculations that involve several different scales. The chart in Figure 17.3 and also the one in Figure 1 in [1120] offer a general view of such analyses. Indeed, a useful review about EDMs can be found in [1120], which updates the review in [1186]. See also [1187, 1188, 1347] and in particular in the case of EDMs of diamagnetic atoms the review in [1189]. As despite a

Downloaded from https://www.cambridge.org/core. UNIVERSIDAD AUTONOMA METROPOLITANA, on 16 Nov 2026 at 21:17:32, subject to the Cambridge Core terms of use, available at https://www.cambridge.org/core/terms. https://doi.org/10.1017/9781139524100.023

few publications involving EDMs I do not consider myself to be an expert in this field, the present section benefited in a very significant manner from these reviews, in particular from [1120, 1186, 1188] and a transparent summary in section 2 of [908]. Also the very recent analysis in [1076] can be strongly recommended. It contains up-to-date hadronic, nuclear, and atomic matrix elements necessary for the phenomenology.

Many details not presented here can be found in these papers and the ones quoted later. I hope that potential readers will find this section to be a useful guide to these reviews and to the rich literature.

Before going into details let us recall the following elementary facts [1120, 1186]. The interaction of a neutral nonrelativistic particle of spin S with magnetic and electric fields can be described by the following Hamiltonian,

$$H = -\mu \vec{B} \cdot \frac{\vec{S}}{S} - d\vec{E} \cdot \frac{\vec{S}}{S} \,. \tag{17.56}$$

Now under the reflection of spatial coordinates, we have

$$P(\vec{B} \cdot \vec{S}) = \vec{B} \cdot \vec{S}, \qquad P(\vec{E} \cdot \vec{S}) = -\vec{E} \cdot \vec{S}. \tag{17.57}$$

Similar under time reflection,

$$T(\vec{B} \cdot \vec{S}) = \vec{B} \cdot \vec{S}, \qquad T(\vec{E} \cdot \vec{S}) = -\vec{E} \cdot \vec{S}. \tag{17.58}$$

Therefore a nonzero electric dipole moment d may exist if and only if both parity and time reversal invariance are broken. Assuming then the CPT theorem, this also implies that the violation of CP is required. The profound difference from other CP-violating phenomena considered in this book is that nonvanishing EDMs do not require simultaneous flavor violation so that flavor-conserving CP-violating interactions are prime sources of them. But as we will discuss later also flavor-violating interactions can generate EDMs.

In the case of a spin-1/2 particle the relativistic generalization of its interaction with the electric field implies the familiar Lagrangian

$$\boxed{\mathcal{L} = -d\frac{i}{2}\overline{\psi}\sigma^{\mu\nu}\gamma_5\psi F_{\mu\nu}.} \tag{17.59}$$

17.3.2 Basic Structure: Nuclear Scale

To see the basic structure of interactions involved eventually in the calculation of EDMs, we do not begin our presentation with high-energy NP or electroweak scale but with the nuclear scale. Subsequently, in Section 17.3.3 we will proceed as in the rest of the book by starting with a fundamental Lagrangian involving elementary fields. Finally, with the help of renormalization group and SMEFT, we will find out how the objects encountered at the nuclear scale are related to the fundamental parameters of a given theory. We follow then [1186] and write down first the relevant CP-odd terms at the nuclear scale:

$$\mathcal{L}_{eff}^{\text{nuclear}} = \mathcal{L}_{\text{edm}} + \mathcal{L}_{\pi NN} + \mathcal{L}_{eN}. \tag{17.60}$$

Downloaded from https://www.cambridge.org/core. UNIVERSIDAD AUTONOMA METROPOLITANA, on 16 Nov 2026 at 21:17:32, subject to the Cambridge Core terms of use, available at https://www.cambridge.org/core/terms. https://doi.org/10.1017/9781139524100.023

The different contributions represent the nucleon (and electron) EDMs,

$$\boxed{\mathcal{L}_{\rm edm} = -\frac{i}{2}\sum_{i=e,p,n} d_i\,\overline{\psi}_i(F\sigma)\gamma_5\psi_i,} \tag{17.61}$$

the CP-odd pion nucleon interactions

$$\boxed{\mathcal{L}_{\pi NN} = \bar{g}^{(0)}_{\pi NN}\bar{N}\tau^a N\pi^a + \bar{g}^{(1)}_{\pi NN}\bar{N}N\pi^0 + \bar{g}^{(2)}_{\pi NN}(\bar{N}\tau^a N\pi^a - 3\bar{N}\tau^3 N\pi^0),} \tag{17.62}$$

and CP-odd electron-nucleon interactions

$$\begin{aligned}\mathcal{L}_{eN} = {} & C^{(0)}_S\bar{e}i\gamma_5 e\bar{N}N + C^{(0)}_P\bar{e}e\bar{N}i\gamma_5 N + C^{(0)}_T\epsilon_{\mu\nu\alpha\beta}\bar{e}\sigma^{\mu\nu}e\bar{N}\sigma^{\alpha\beta}N \\ & + C^{(1)}_S\bar{e}i\gamma_5 e\bar{N}\tau^3 N + C^{(1)}_P\bar{e}e\bar{N}i\gamma_5\tau^3 N + C^{(1)}_T\epsilon_{\mu\nu\alpha\beta}\bar{e}\sigma^{\mu\nu}e\bar{N}\sigma^{\alpha\beta}\tau^3 N.\end{aligned} \tag{17.63}$$

We should warn the reader that at a few places the notation of couplings in [1186] and [1120], that we use heavily here, differs from each other. In particular,

$$\bar{g}^{(0)}_{\pi NN} = \bar{g}^{(0)}_{\pi}, \qquad \bar{g}^{(1)}_{\pi NN} = \bar{g}^{(1)}_{\pi}, \qquad \bar{g}^{(2)}_{\pi NN} = -\bar{g}^{(2)}_{\pi} \tag{17.64}$$

for [1186] and [1120], respectively. The *bar* stresses the CP-odd character of the couplings. Relations to notations of couplings in other reviews are collected in table 4 of [1120].

Even if at first sight one would think that only elementary d_i would contribute to EDMs of atoms and molecules, this is in reality not the case as also the CP-odd pion nucleon iterations and CP-odd electron-nucleon couplings can contribute. This makes the extraction of the elementary EDMs d_e and $d_{n,p}$ a challenge.

The basic entries in these formulas are then

$$d_e,\quad d_{n,p},\quad \bar{g}^{(0)}_{\pi NN},\quad \bar{g}^{(1)}_{\pi NN},\quad \bar{g}^{(2)}_{\pi NN},\quad C^{(0)}_S,\quad C^{(1)}_S,\quad C^{(0)}_P,\quad C^{(1)}_P,\quad C^{(0)}_T,\quad C^{(1)}_T. \tag{17.65}$$

While the neutron EDM d_n is already an observable, the other preceding quantities enter the formulas for measureable EDMs of atoms and molecules. Our goal will be the presentation of a general formula for the EDM d_A of an arbitrary atom in terms of the objects in (17.65) as given in [1120]. But as seen in Section 17.3.4, this formula is rather involved, and it is useful to give first some background behind it and to stress which parts can be calculated in perturbation theory and for which nonperturbative methods have to be used.

Observable EDMs

As discussed in [1186] it is convenient to classify the EDM searches into three main categories, distinguished by the dominant physics that would induce the EDMs. These categories are

Downloaded from https://www.cambridge.org/core. UNIVERSIDAD AUTONOMA METROPOLITANA, on 16 Nov 2026 at 21:17:32, subject to the Cambridge Core terms of use, available at https://www.cambridge.org/core/terms. https://doi.org/10.1017/9781139524100.023

- the EDMs of *paramagnetic* atoms and molecules involving electron EDM, d_e, with the main actor being the atomic EDM of the thallium atom (Tl),
- the EDMs of *diamagnetic* atoms with the EDM of the mercury atom (^{199}Hg) playing presently the main role, and
- the EDMs of hadrons with particular emphasize put on EDMs of nucleons: d_n and d_p.

EDMs of Paramagnetic Atoms

The EDMs of paramagnetic atoms are governed by the EDM of one unpaired electron, that is d_e. At the nonrelativistic level, this would not be possible due to the Schiff shielding theorem. Indeed, because the atom is neutral, any applied electric field will be shielded and so an EDM of the unpaired electron will not induce an atomic EDM. But this theorem is violated by relativistic effects, in particular for atoms with a large atomic number and molecules. As an example, for the paramagnetic atoms one finds [1190]

$$d_{\text{para}}(d_e) \sim 10 \frac{Z^3 \alpha^2}{J(J+1/2)(J+1)^2} d_e, \tag{17.66}$$

up to numerical $O(1)$ factors, with J the angular momentum and Z the atomic number.

The large enhancement factor for large Z allows to probe the electron EDM very efficiently. Beyond d_e CP-odd electron-nucleon interactions may also play a significant role, in particular the couplings $C_S^{(0)}$ and $C_S^{(1)}$, because they involve the spin of the electron and are enhanced by the large nucleon number in heavy atoms. As an example, we quote the expression for the EDM of the thallium atom that currently provides the best constraints on fundamental flavor-diagonal CP violation. A number of atomic calculations established the relation between the EDM of thallium, d_e, and the CP-odd electron-nucleon couplings $C_S^{(0)}$ and $C_S^{(1)}$ [1190]

$$d_{\text{Tl}} = -585 d_e - e\ 43\ \text{GeV} \times (C_S^{(0)} - 0.2\, C_S^{(1)}). \tag{17.67}$$

The relevant atomic numerical factors are known to within 10–20% [1190]. Further examples will be given later. But we already see that to extract the electron EDM d_e from d_{Tl} requires the knowledge of numerical factors resulting from atomic calculations and also of the coefficients $C_S^{(0)}$ and $C_S^{(1)}$ that can be generated by NP but also involve some nonperturbative uncertainties.

EDMs of Diamagnetic Atoms

The total electron angular momentum in diamagnetic atoms equals to zero. This time the Schiff theorem is violated through a net misalignment between the distribution of charge and EDM (i.e., first and second moments) in the nucleus. But unfortunately the induced atomic EDM is considerably suppressed relative to the underlying EDM of the nucleus. This time also the calculations are much more involved requiring input from QCD as well

Downloaded from https://www.cambridge.org/core. UNIVERSIDAD AUTONOMA METROPOLITANA, on 16 Nov 2026 at 21:17:32, subject to the Cambridge Core terms of use, available at https://www.cambridge.org/core/terms. https://doi.org/10.1017/9781139524100.023

as nuclear and atomic physics. Thus generally the EDMs of the diamagnetic atoms receive contributions from many interactions

$$d_{\rm dia} = d_{\rm dia}(S[\bar{g}_{\pi NN}], d_N, C_S, C_P, C_T, d_e). \tag{17.68}$$

Here S is the Schiff moment. Its computation is a nontrivial nuclear many-body problem. It can be written generally as follows

$$S[\bar{g}_{\pi NN}] = a_0\, g\bar{g}^{(0)} + a_1 g\bar{g}^{(1)} + a_2 g\bar{g}^{(2)} \tag{17.69}$$

where $g \equiv g_{\pi NN}$ is the CP-even pion-nucleon coupling, and $\bar{g}^{(i)} \equiv \bar{g}^{(i)}_{\pi NN}$ denote the CP-odd couplings entering (17.62). As an example, one finds for the mercury atom [1191]

$$S(^{199}{\rm Hg}) = -0.0004 g\bar{g}^{(0)} - 0.055 g\bar{g}^{(1)} + 0.009 g\bar{g}^{(2)}\ e\ {\rm fm}^3. \tag{17.70}$$

We note very strong suppression factors.

Keeping only the isovector pion-nucleon coupling and $C_S^{(0)}$ one finds then for the mercury EDM [1186]

$$d_{\rm Hg} = -(1.8\times 10^{-4}\ {\rm GeV}^{-1}) e\, \bar{g}^{(1)}_{\pi NN} + 10^{-2} d_e + (3.5\times 10^{-3}\ {\rm GeV}) e\, C_S^{(0)}. \tag{17.71}$$

Neutron and Proton EDMs

Neutron EDM can be searched for directly with ultracold neutron technology, and its calculation does not involve any atomic or nuclear physics. But similar to many observables considered in this book, it requires good control over nonperturbative QCD effects to find the dependence of d_n on CP-odd sources at the quark-gluon level. As we deal now with a baryon instead of a meson such calculations are much more demanding than is the case of K and B physics. Yet, currently d_n provides one of the strongest constraints on new CP-violating physics, and one should make all efforts to improve the precision of the theory.

17.3.3 Electroweak Scale, SMEFT, and RG Evolution

We have just described the basic structure of EDMs at the nuclear scales. While in principle we could next discuss the *hadronic* scale, I find it strategically better to present first what happens at the electroweak scale because this was the starting point for all processes discussed in this book. Thus at the electroweak scale of $O(M_W)$ after $W^\pm$, Z^0, t, Higgs particle, and all heavy new particles have been integrated out, we will have an effective Hamiltonian written as the sum of products of WCs and local operators. The construction of this Hamiltonian proceeds as in previous chapters, and we make only few comments:

- In a given NP model one integrates out heavy particles at a given scale, which could be many orders of magnitude higher than the EW scale. This then implies the presence of local operators multiplied by corresponding WCs. Which operators are relevant and which not depends on the NP model considered and on the next step.

Downloaded from https://www.cambridge.org/core. UNIVERSIDAD AUTONOMA METROPOLITANA, on 16 Nov 2026 at 21:17:32, subject to the Cambridge Core terms of use, available at https://www.cambridge.org/core/terms. https://doi.org/10.1017/9781139524100.023

- This next step is the RG evolution to the EW scale crossing generally various thresholds at which some of new particles are integrated out. The SMEFT technology should be used here so that in addition to QCD effects top Yukawa effects, and EW effects play some role. The RG evolution generates new operators through mixing, and in addition threshold corrections can have an impact on WCs. There is an extensive literature on the relevant calculations of anomalous dimensions that was already given in Section 14.1. In the context of EDMs a very transparent presentation is given in [781], where references to the relevant papers can be found. See also table 5 in [1120].
- Next after the integration of heavy SM particles that is $W^{\pm}$, Z^0, t, and the Higgs particle one continues the RG evolution to hadronic scales at which the relevant hadronic matrix elements of resulting operators are evaluated in QCD. The RG evolution involves now QCD and QED effects.
- Finally, in many cases nuclear and atomic calculations have to be performed to connect fundamental parameters of a given theory to the low-energy parameters in (17.65). Various methods are critically reviewed in sections 3 and 4 in [1120].

If a given NP model is specified this analysis is rather straightforward even if often tedious. In particular only certain operators are relevant in a given model, and their WCs can be calculated in terms of the fundamental parameters. If the number of these parameters is small, some relations between these coefficients characteristic for a given model are present.

On the other hand, if a model is not specified it is a common practice these days to use the SMEFT that we presented in Section 14.1 and applied it already to several processes. The advantage of this approach over a specific model is its generality. The disadvantage is the appearance of many operators with arbitrary WCs even if in certain situations some relations between them are implied by the invariance under the SM gauge symmetry. The list of operators relevant for EDMs will be given soon.

The main sources of CPV are then encoded in

$$\mathcal{L}_{\rm CPV} = \mathcal{L}_{\rm CKM} + \mathcal{L}_{\bar\theta} + \mathcal{L}^{\rm eff}_{\rm BSM}, \tag{17.72}$$

where the first term on the r.h.s. is the standard CKM contribution and the second term is the so-called QCD θ-term

$$\boxed{\mathcal{L}_{\bar\theta} = -\frac{g_3^2}{16\pi^2}\bar\theta\,{\rm Tr}\left(G^{\mu\nu}\tilde G^{\mu\nu}\right), \qquad \tilde G^{\mu\nu} = \frac{1}{2}\epsilon^{\mu\nu\alpha\beta}G_{\alpha\beta}\,,} \tag{17.73}$$

where $\tilde G^{\mu\nu}$ is the dual to the gluon field strength $\tilde G^{\mu\nu}$.

The last term in (17.72) representing dimension-6 CPV operators is given generally as follows

$$\boxed{\mathcal{L}^{\rm eff}_{\rm BSM} = \frac{1}{\Lambda^2}\sum_i \alpha_i^{(n)} O_i^{(6)}.} \tag{17.74}$$

Downloaded from https://www.cambridge.org/core. UNIVERSIDAD AUTONOMA METROPOLITANA, on 16 Nov 2026 at 21:17:32, subject to the Cambridge Core terms of use, available at https://www.cambridge.org/core/terms. https://doi.org/10.1017/9781139524100.023

We encountered this expression already in Section 14.1. These operators can be generated by BSM physics at many different scales, but here for simplicity we just exhibit only one scale Λ. The relevant operators are listed in tables 2 and 3 in [1120] and can also be found in Section 14.1. The operators that involve the Higgs field, $W^{\mu\nu}$, $B^{\mu\nu}$ are only relevant for the normalization of the corresponding WCs. But what really matters are the resulting low-energy interactions that play the role in the evaluation of EDMs. Let us discuss them one by one.

Dimension-6 Operators

Let us then list the most important dimension-6 operators generated by BSM physics that are relevant for EDMs. Adjusting the notation of [1120] to the one of Section 14.1 we have

$$Q_{uG} = (\bar{q}\sigma^{\mu\nu}T^A u_R)\tilde{\phi}G^A_{\mu\nu}, \qquad Q_{dG} = (\bar{q}\sigma^{\mu\nu}T^A d_R)\phi G^A_{\mu\nu}, \tag{17.75}$$

$$Q_{eW} = (\bar{\ell}\sigma^{\mu\nu}e_R)\tau^I\phi W^I_{\mu\nu}, \qquad Q_{eB} = (\bar{\ell}\sigma^{\mu\nu}e_R)\tau^I\phi B_{\mu\nu}, \tag{17.76}$$

$$Q_{uW} = (\bar{q}\sigma^{\mu\nu}u_R)\tau^I\phi W^I_{\mu\nu}, \qquad Q_{uB} = (\bar{q}\sigma^{\mu\nu}u_R)\tau^I\phi B_{\mu\nu}, \tag{17.77}$$

$$Q_{dW} = (\bar{q}\sigma^{\mu\nu}d_R)\tau^I\phi W^I_{\mu\nu}, \qquad Q_{dB} = (\bar{q}\sigma^{\mu\nu}d_R)\tau^I\phi B_{\mu\nu}, \tag{17.78}$$

$$Q_{\tilde{G}} = f^{ABC}\tilde{G}^{A\nu}_{\mu}G^{B\rho}_{\nu}G^{C\mu}_{\rho} \tag{17.79}$$

and *four-fermion operators* with

$$Q^{(1)}_{quqd} = (\bar{q}^j u_R)\epsilon_{jk}(\bar{q}^k d_R), \qquad Q^{(8)}_{quqd} = (\bar{q}^j T^A u_R)\epsilon_{jk}(\bar{q}^k T^A d_R), \tag{17.80}$$

$$Q^{(1)}_{lequ} = (\bar{\ell}^j e_R)\epsilon_{jk}(\bar{q}^k u_R), \qquad Q^{(3)}_{lequ} = (\bar{\ell}^j \sigma^{\mu\nu} e_R)\epsilon_{jk}(\bar{q}^k \sigma^{\mu\nu} u_R), \tag{17.81}$$

$$Q_{ledq} = (\bar{\ell}^j e_R)(\bar{d}_R q^j). \tag{17.82}$$

It should be emphasized that the index e stands here not only for the electron but also for μ and τ. Similar for d and u. In particular one can consider the EDM of the top quark [781, 1192], and we will return to this case at the end of this section.

First, after the electroweak symmetry breaking Q_{qG} gives rise to the quark chromo-electric dipole moment (CEDM) interaction

$$\boxed{\mathcal{L}^{\rm CEDM} = -i\sum_q \tilde{d}_q \frac{g_3}{2}\bar{q}\sigma^{\mu\nu}T^A\gamma_5 q G^A_{\mu\nu}, \qquad \tilde{d}_q = -\frac{\sqrt{2}}{v}\left(\frac{v}{\Lambda}\right)^2 {\rm Im}C_{qG},} \tag{17.83}$$

where $v = 246\,{\rm GeV}$ and C_{qG} is the WC of Q_{qG}. C_{qG} can be calculated in a given BSM model.

Next, Q_{fW} and Q_{fB} generate the elementary fermion EDM interactions

$$\boxed{\mathcal{L}^{\rm EDM} = -i\sum_f \frac{d_f}{2}\bar{f}\sigma^{\mu\nu}\gamma_5 f F_{\mu\nu}, \qquad d_f = -e\frac{\sqrt{2}}{v}\left(\frac{v}{\Lambda}\right)^2 {\rm Im}C_{f\gamma},} \tag{17.84}$$

Downloaded from https://www.cambridge.org/core. UNIVERSIDAD AUTONOMA METROPOLITANA, on 16 Nov 2026 at 21:17:32, subject to the Cambridge Core terms of use, available at https://www.cambridge.org/core/terms. https://doi.org/10.1017/9781139524100.023

where

$$\mathrm{Im}C_{f\gamma} = \mathrm{Im}C_{fB} + 2I_3^f \,\mathrm{Im}C_{fW}. \tag{17.85}$$

Here I_3^f is the third component of the weak isospin for the fermion f. Again $C_{f\gamma}$ can be calculated in a given BSM model.

Inserting $v = 246\,\mathrm{GeV}$ into (17.83) and (17.84) one finds [1120]

$$\tilde{d}_q = -(1.13\times 10^{-3}\ \mathrm{fm})\left(\frac{v}{\Lambda}\right)^2 \mathrm{Im}C_{qG}, \qquad d_f = -(1.13\times 10^{-3}\ \mathrm{fm})\left(\frac{v}{\Lambda}\right)^2 \mathrm{Im}C_{f\gamma}. \tag{17.86}$$

As stressed in [1120] the presence of the CEDM and EDM operators, similar to operators governing $b \to s\gamma$ decay and fermion magnetic moments, requires chirality flip, and consequently their WCs are proportional to the relevant fermion mass

$$m_f = \frac{v}{\sqrt{2}} Y_f, \tag{17.87}$$

with Y_f being the Yukawa coupling. For this reason it is useful to work also with $\tilde{\delta}_q$ and δ_f defined by [1120]

$$\mathrm{Im}\, C_{qG} \equiv Y_q \tilde{\delta}_q, \qquad \mathrm{Im}\, C_{f\gamma} \equiv Y_f \delta_f, \tag{17.88}$$

so that

$$\tilde{d}_q = -\frac{2m_q}{v^2}\left(\frac{v}{\Lambda}\right)^2 \tilde{\delta}_q, \qquad d_f = -e\frac{2m_q}{v^2}\left(\frac{v}{\Lambda}\right)^2 \delta_f. \tag{17.89}$$

Next the so-called Weinberg three-gluon operator $Q_{\tilde{G}}$ gives

$$\boxed{\mathcal{L}^{\tilde{G}}_{\mathrm{CPV}} = g_3 \frac{C_{\tilde{G}}}{\Lambda^2} f^{ABC} \tilde{G}^{A\nu}_{\mu} G^{B\rho}_{\nu} G^{C\mu}_{\rho}.} \tag{17.90}$$

Among four-fermion operators one should distinguish between the semileptonic and hadronic ones. The CPV *semileptonic interactions* are described by

$$\mathcal{L}^{eq}_{\mathrm{CPV}} = i\frac{\mathrm{Im}C_{ledq}}{2\Lambda^2}[\bar{e}\gamma_5 e\, \bar{d}d - \bar{e}e\, \bar{d}\gamma_5 d] - i\frac{\mathrm{Im}C^{(1)}_{lequ}}{2\Lambda^2}[\bar{e}\gamma_5 e\, \bar{u}u + \bar{e}e\, \bar{u}\gamma_5 u] \tag{17.91}$$

$$- \frac{\mathrm{Im}C^{(3)}_{lequ}}{2\Lambda^2}\epsilon_{\mu\nu\alpha\beta}\bar{e}\sigma^{\mu\nu} e\, \bar{u}\sigma^{\alpha\beta} u \tag{17.92}$$

and the CPV *hadronic interactions* by

$$\mathcal{L}^{qq}_{\mathrm{CPV}} = i\frac{g_3^2 \mathrm{Im}C^{(1)}_{quqd}}{2\Lambda^2}[\bar{u}\gamma_5 u \bar{d}d + \bar{u}u\, \bar{d}\gamma_5 d - \bar{d}\gamma_5 u\, \bar{u}d - \bar{d}u\, \bar{u}\gamma_5 d] \tag{17.93}$$

$$+ i\frac{g_3^2 \mathrm{Im}C^{(8)}_{quqd}}{2\Lambda^2}[\bar{u}\gamma_5 T^A u\, \bar{d}T^A d + \bar{u}T^A u\, \bar{d}\gamma_5 T^A d \tag{17.94}$$

$$- \bar{d}\gamma_5 T^A u\, \bar{u}T^A d - \bar{d}T^A u\, \bar{u}\gamma_5 T^A d]. \tag{17.95}$$

Downloaded from https://www.cambridge.org/core. UNIVERSIDAD AUTONOMA METROPOLITANA, on 16 Nov 2026 at 21:17:32, subject to the Cambridge Core terms of use, available at https://www.cambridge.org/core/terms. https://doi.org/10.1017/9781139524100.023

The coefficients C_i are the WCs of the four-fermion operators listed earlier.

It should be emphasized that in left-right symmetric models the chirality flip can be generated in a different manner and still other contributions with different flavor structure are possible:

$$\mathcal{L}^{\rm eff}_{\rm LR,CPV} = \quad i\frac{{\rm Im}C_{\phi ud}}{3\Lambda^2}\{\bar{u}u\,\bar{d}\gamma_5 d - \bar{u}\gamma_5 u\,\bar{d}d + 3[\bar{u}T^A u\,\bar{u}\gamma_5 T^A d - \bar{u}\gamma_5 T^A u\,\bar{d}T^A d]\}. \tag{17.96}$$

θ Term

It is time to discuss briefly the θ-term, which enters the Lagrangian in (17.73). This dim-4 term is allowed by all symmetries of the SM but violates both CP and T. It is by now constrained to be at most 10^{-10}, precisely because of the nonobservation of the permanent EDM of the mercury atom.[1] The unnatural small value of this term signals the so-called strong CP-problem. One of its solutions is the increase of the Higgs system with additional symmetry, Peccei–Quinn (PQ) symmetry $\mathrm{U}(1)_{PQ}$ [1193, 1194], which allows to eliminate this term. The spontaneous breakdown of this symmetry implies the existence of a pseudoscalar Goldstone boson, the axion [1195, 1196], that has not been observed. Other solutions to strong CP problem without the PQ symmetry have been presented in [1197, 1198]. A recent review of this subject with implications for cosmology can be found in [1199]. Also the updates in PDG are useful in this respect.

Actually, what really enters physical expressions is not θ but

$$\bar{\theta} = \theta + \arg\det(Y_u Y_d), \tag{17.97}$$

with Y_i being Yukawa couplings. Thus this term is connected with quark masses, and the second term arises after the phases of all quark fields have been redefined. However, in some BSM scenarios radiative corrections to quark masses can generate unacceptably large contributions to $\bar{\theta}$ implying severe constraints on model parameters unless some symmetries like the PQ one is present.

The presence of the $\bar{\theta}$ term complicates the search for NP in the case of nucleons and diamagnetic systems, but measuring deviations in several systems one could disentangle NP from this term [1200].

Additional Remarks on EDMs in SMEFT

The formfactors listed in Table 17.4 for $f = i$ can be directly used to calculate EDMs of charged leptons [795]

$$\boxed{d_{l_i} = -\frac{1}{\Lambda^2}{\rm Im}[F^{ii}_{TR}].} \tag{17.98}$$

[1] Apparently as stressed in [1188] this bound can be relaxed in a global analysis by a few orders of magnitude.

Downloaded from https://www.cambridge.org/core. UNIVERSIDAD AUTONOMA METROPOLITANA, on 16 Nov 2026 at 21:17:32, subject to the Cambridge Core terms of use, available at https://www.cambridge.org/core/terms. https://doi.org/10.1017/9781139524100.023

A very clear presentation of the application of SMEFT and RG ideas to EDMs is given in [1076]. Although it is given in the context of specific LQ models, it shows transparently many different aspects of the physics of EDMs and can be strongly recommended.

17.3.4 General Formula

With the information about various contributions at hand, we are ready to write down a formula for a general atomic or molecular EDM d_A in terms of d_e, d_N, the nuclear Schiff moment S, and the coefficients $C^{(0)}_{S,P,T}$ and $C^{(1)}_{S,P,T}$. These are the basic entries in (17.65) with $\bar{g}^{(i)}_{\pi NN}$ hidden in S as given in (17.69). Rewriting (5.171) and (5.172) of [1120] in terms of these coefficients we have then

$$d_A = \rho^e_A\, d_e + \sum_{N=p,n} \rho^N_Z\, d_N + \kappa_S S - \left[k^{(0)}_S C^{(0)}_S + k^{(1)}_P C^{(1)}_P\right] \tag{17.99}$$

$$+ \left[k^{(1)}_S C^{(1)}_S + k^{(0)}_P C^{(0)}_P\right] - \left[k^{(0)}_T C^{(0)}_T + k^{(1)}_T C^{(1)}_T\right]. \tag{17.100}$$

In all these contributions one can exhibit $(v/\Lambda)^2$ terms. Indeed we have first

$$\rho^e_A\, d_e = \beta^{e\gamma}_A \left(\frac{v}{\Lambda}\right)^2 \mathrm{Im}C_{e\gamma}, \tag{17.101}$$

$$d_N = \alpha_N \bar{\theta} + \left(\frac{v}{\Lambda}\right)^2 \sum_k \beta^{(k)}_N \mathrm{Im}C_k, \tag{17.102}$$

$$\bar{g}^{(i)} = \lambda_{(i)} \bar{\theta} + \left(\frac{v}{\Lambda}\right)^2 \sum_k \gamma^{(k)}_{(i)} \mathrm{Im}C_k, \tag{17.103}$$

and $\bar{g}^{(i)} \equiv \bar{g}^{(i)}_{\pi NN}$ inserted into (17.69) allows to express also Schiff moment in terms of $(v/\Lambda)^2$. The coefficients α_N, $\beta^{(k)}_N$, $\lambda_{(i)}$, and $\gamma^{(k)}_{(i)}$ are subject to hadronic uncertainties and result from the calculations of hadronic matrix elements. This is the place where hadronic scales enter the game.

Next we have

$$C^{(0)}_S = -g^{(0)}_S \left(\frac{v}{\Lambda}\right)^2 \mathrm{Im}C^{(-)}_{eq}, \qquad C^{(1)}_S = g^{(1)}_S \left(\frac{v}{\Lambda}\right)^2 \mathrm{Im}C^{(+)}_{eq}, \tag{17.104}$$

$$C^{(0)}_P = g^{(0)}_P \left(\frac{v}{\Lambda}\right)^2 \mathrm{Im}C^{(+)}_{eq}, \qquad C^{(1)}_P = -g^{(1)}_P \left(\frac{v}{\Lambda}\right)^2 \mathrm{Im}C^{(-)}_{eq}, \tag{17.105}$$

$$C^{(0)}_T = -g^{(0)}_T \left(\frac{v}{\Lambda}\right)^2 \mathrm{Im}C^{(3)}_{lequ}, \qquad C^{(1)}_S = -g^{(1)}_T \left(\frac{v}{\Lambda}\right)^2 \mathrm{Im}C^{(3)}_{lequ}, \tag{17.106}$$

where

$$C^{(\pm)}_{eq} = C_{ledq} \pm C^{(1)}_{lequ} \tag{17.107}$$

Downloaded from https://www.cambridge.org/core. UNIVERSIDAD AUTONOMA METROPOLITANA, on 16 Nov 2026 at 21:17:32, subject to the Cambridge Core terms of use, available at https://www.cambridge.org/core/terms. https://doi.org/10.1017/9781139524100.023

and $g^{(i)}_{S,P,T}$ are the isoscalar and isovector formfactors in the limit of isospin symmetry

$$\frac{1}{2}\langle N|[\bar{u}\Gamma u + \bar{d}\Gamma d]|N\rangle \equiv g^{(0)}_\Gamma \bar{\psi}_N \Gamma \psi_N, \qquad \frac{1}{2}\langle N|[\bar{u}\Gamma u - \bar{d}\Gamma d]|N\rangle \equiv g^{(0)}_\Gamma \bar{\psi}_N \Gamma \tau_3 \psi_N, \tag{17.108}$$

where $\Gamma = 1, \gamma_5, \sigma_{\mu\nu}$.

The coefficients ρ^N_Z, κ_S, $k^{(0)}_{S,P,T}$, $k^{(1)}_{S,P,T}$, $g^{(0)}_{S,P,T}$, and $g^{(1)}_{S,P,T}$ are subject to nonperturbative uncertainties. A compilation of their values can be found in [1120]. In that paper also applications of this formula and examples can be found. Here we just quote the result for *diamagnetic* atoms presented in [1188]:

$$d_A = \sum_{N=p,n} \rho^N_Z \, d_N + \kappa_S S - \left[k^{(0)}_T C^{(0)}_T + k^{(1)}_T C^{(1)}_T\right], \tag{17.109}$$

with the various entries given in eqs. (II.14)–(II.16) of that paper.

17.3.5 General Picture and New Physics

One can then ask which short-distance scales can be probed by EDMs. As discussed in [1120] by naive dimension analysis EDMs probe a NP scale of several TeV. This assumes order one CP-violating phases $\phi_{\rm CP}$ for the electron EDM that arises at one loop order:

$$d_e \approx e\frac{m_e}{\Lambda^2}\frac{\alpha_e}{4\pi}\sin\phi_{\rm CP} \approx \frac{1}{2}\left(\frac{1\ \text{TeV}}{\Lambda}\right)^2 \sin\phi_{\rm CP}\cdot 10^{-26} e\,\text{cm}\,. \tag{17.110}$$

Recently, the upper bound on d_e has been improved by an order of magnitude with respect to the previous bound in [1201] and reads [1177]

$$|d_e| \leq 1.1\cdot 10^{-29} e\,\text{e cm}. \tag{17.111}$$

This then implies for the CP-violating phase $|\sin\phi_{\rm CP}| \lesssim \left(\frac{\Lambda}{15\ \text{TeV}}\right)^2$.

The scale of NP can be even higher for the neutron and ^{199}Hg EDMs as they are sensitive to the chromo-magnetic EDM, which enters with a factor of α_s rather than the fine structure constant α_e. As one can see from (17.110) the sensitivity to the NP scale goes as $1/\Lambda^2$, whereas in many other cases such as lepton flavor violation the sensitivity goes as $1/\Lambda^4$. Future EDM measurements aim to improve their sensitivity by approximately two orders of magnitude, which will then push the mass scale sensitivity into the (30–100) TeV range.

Flavor-diagonal CP violating phases as needed for electroweak baryogenesis can be strongly constrained by EDMs. In the MSSM, for example, this requires rather heavy first- and second-generation sfermions but at the same time light electroweak gauginos below one TeV as well as a subset of the third-generation sfermions (see [1202] for details). However, as can be deduced from the plots in [1203] the improved bound on d_e in (17.111) nearly excludes this possibility. While the bino-driven baryogenesis analyzed in [1204] is still allowed by this new measurements, it further constraints this scenario.

A new and largely unexplored direction for electroweak baryogenesis is flavor nondiagonal CPV that would enter the B or D meson systems [1205–1207]. Flavor nondiagonal CP violation is far less susceptible to EDM constraints than flavor-diagonal

Downloaded from https://www.cambridge.org/core. UNIVERSIDAD AUTONOMA METROPOLITANA, on 16 Nov 2026 at 21:17:32, subject to the Cambridge Core terms of use, available at https://www.cambridge.org/core/terms. https://doi.org/10.1017/9781139524100.023

phases because it arises at multiloop order. In the SM, for example, it is a two-loop effect that involves the one-loop CP-violating penguin operator and a hadronic loop with two $\Delta S = 1$ weak interactions.

Until now our discussion was quite general, and it is time to stress which contributions are largest. We stated already that in the SM the EDMs are tiny. When new sources of CP violation are present in NP models, large contributions to EDMs can be generated, and unless some suppression mechanisms are invoked even one-loop contributions are too large to satisfy the present upper bounds. Once these suppressions are invoked the question arises of whether two-loop diagrams could be important. In fact, as realized first by Weinberg [1208], in a wide class of models two-loop diagrams generating Weinberg-operator can be a very important contribution. In fact, these contributions would be by far dominant if they were not strongly suppressed by RG effects. Another type of two-loop diagrams are Barr–Zee(-type) diagrams [1209–1211] that are often dominant in models with new heavy scalars.

It is not possible to review the studies of EDMs in various extensions of the SM. A brief review of EDMs in supersymmetric models, in models with extended gauge symmetry, in particular left-right symmetric models and in models with extra dimensions can be found in [1120]. Studies of EDMs in 2HDM models with flavor blind phases can be found in [908, 909] and supersymmetry [1212], where further references to the rich literature can be found. A general description [1213] of the search for NP with the EDMs can be found in [1213]. The implications of the improved upper bound on d_e [1177] on various NP models has been studied in [1214]. Correlations between tautonic B meson decays like $B \to \tau\nu$, $B \to D^{(*)}\tau\nu$, $B \to \pi\tau\nu$, and EDMs, in particular the one of the neutron have been investigated in the context of S_1 LQ model in [1215].

As EDMs are sensitive to CP-violating phases, they should provide bounds on new phases in the Yukawa couplings of quarks to the Higgs boson. Indeed, as shown in [1216–1219] these bounds could be rather stringent. The same is true for CP-phases in leptoquark models as demonstrated for R_2 and S_1 models in [1076, 1220]. In fact, generally the bounds on EDMs could have an impact on the explanations of various anomalies, like B physics anomalies, as stressed recently in [719, 1076, 1200, 1221]. The correlation between the CP violation in the Kaon sector, in particular ε'/ε, with the neutron EDM in the context of left-right symmetric models, has been analyzed in [1318]. Further references to older discussions of this important issue can be found in these papers.

17.3.6 EDMs of Heavy Fermions

As we have seen until now, the most stringent limits for EDMs stem presently from experiments with heavy atoms and molecules as well as neutrons, built from first-generation fermions. However, there is the distinct possibility that NP affects primarily heavier fermions. CP-violating moments of these heavier fermions have been investigated in the past, and improvements are possible at current and future colliders. However, these rather direct limits are typically many orders of magnitude weaker than those for the moments of first-generation fermions. Recently it has been demonstrated in several papers

Downloaded from https://www.cambridge.org/core. UNIVERSIDAD AUTONOMA METROPOLITANA, on 16 Nov 2026 at 21:17:32, subject to the Cambridge Core terms of use, available at https://www.cambridge.org/core/terms. https://doi.org/10.1017/9781139524100.023

that much more stringent indirect limits on the EDMs, chromo-EDMs, and weak dipole moments of heavy particles like charm, beauty, and top quarks, as well as tau lepton and the muon, can be obtained from existing high-precision measurements with atoms, molecules, and neutrons. In particular in [781, 1192, 1222–1224] bounds on d_t from the bounds on neutron's EDM d_n have been derived. Even stronger constraints result from the bounds on d_e and when the bounds on d_n and d_e are simultaneously considered [1192]:

$$|d_t| \leq 1.3 \times 10^{-19}\,\text{e cm}. \tag{17.112}$$

With future improved bounds on d_e, d_n, and d_p this bound could be improved by two orders of magnitude.

Here I would like to describe the basic structure of a recent study by Martin Jung, Emilie Passemar, and myself that generalizes the analyses just mentioned with the aim to constrain the EDMs of all quarks and leptons beyond d, u, and e that is also the (s, c, b) and (μ, τ).

This is an arena for the application of the SMEFT and the related RG technology, which we presented at length in Chapter 14. To this end we postulate the existence of the operators at dimension-6 involving heavy fermions at a high-energy scale Λ that are responsible for EDMs of these fermions. We then investigate RG-induced effects of these new operators on observables at lower energies, like the EDMs of atoms, molecules from which d_e can be extracted and of the neutron and proton. The determination of the dominant mechanism for a given fermion is complicated by the presence of various hierarchies in couplings, masses, mixing angles, hadronic matrix elements, and loop factors. The possible contributions enter at one, two, and three loops. This is illustrated in Table 17.8, where q_i are electric fermion charges and $N_C = 3$ the number of colors. We will list the main patterns in this table after presenting formulas behind these results.

In addition to the evolution of the SMEFT coefficients, which can be performed perturbatively, the connection to measured observables, as we have seen earlier, requires the matching onto hadronic quantities, which involves matrix elements at the atomic, QCD, and nuclear levels, often involving sizable theoretical uncertainties. These steps finally result in expressions for observables in terms of NP coefficients involving heavy fermions.

More explicitly, the CP-violating dipole moments of a fermion f (quark or lepton), defined via

$$\mathcal{L}_f \supset -\frac{i}{2}\left(d_f^\gamma \bar{f}\sigma^{\mu\nu}\gamma_5 f F_{\mu\nu} + d_f^Z \bar{f}\sigma^{\mu\nu}\gamma_5 f Z_{\mu\nu} + g_s \tilde{d}_q \bar{q}\sigma^{\mu\nu}\gamma_5 q G_{\mu\nu}\right), \tag{17.113}$$

are related to the coefficients of the SMEFT (in the mass eigenbasis) as follows:

$$d^\gamma_{f\in D,E} = -\sqrt{2}ev\,\text{Im}\left[\frac{C_{fB}}{g_1} - \frac{C_{fW}}{g_2}\right], \qquad d^\gamma_{f\in U} = -\sqrt{2}ev\,\text{Im}\left[\frac{C_{fB}}{g_1} + \frac{C_{fW}}{g_2}\right], \tag{17.114}$$

$$d^Z_{f\in D,E} = -\sqrt{2}ev\,\text{Im}\left[-\frac{C_{fB}}{g_2} - \frac{C_{fW}}{g_1}\right], \qquad d^Z_{f\in U} = -\sqrt{2}ev\,\text{Im}\left[-\frac{C_{fB}}{g_2} + \frac{C_{fW}}{g_1}\right], \tag{17.115}$$

$$\tilde{d}_{q\in U,D} = -\frac{\sqrt{2}v}{g_s}\,\text{Im}\,C_{qG}. \tag{17.116}$$

Here E, D, U refer to the corresponding families, i.e., $E = \{e, \mu, \tau\}$, $D = \{d, s, b\}$, and $U = \{u, c, t\}$. C_{fX} stand here for the corresponding entry on the diagonal of the coefficient

Downloaded from https://www.cambridge.org/core. UNIVERSIDAD AUTONOMA METROPOLITANA, on 16 Nov 2026 at 21:17:32, subject to the Cambridge Core terms of use, available at https://www.cambridge.org/core/terms. https://doi.org/10.1017/9781139524100.023

matrix, e.g., $C_{cB} = (C_{uB})_{22}$. We do not consider sizable nondiagonal entries in the following, corresponding to large flavor-changing neutral currents at tree-level.

On the other hand, we recall that the relevant Lagrangian at low energies (~ 1 GeV) can be written as follows:

$$\mathcal{L}_{\text{low}} = \sum_{\substack{f,f'=u,d,s,e,\mu \\ q=u,d,s}} \left[-\frac{i}{2} d_f^{\gamma} \bar{f} \sigma^{\mu\nu} \gamma_5 f F_{\mu\nu} - \frac{i}{2} g_s \tilde{d}_q \bar{q} \sigma^{\mu\nu} \gamma_5 q G_{\mu\nu} + C_{ff'} O_{ff'} \right] + C_W O_W, \tag{17.117}$$

where $O_{ff'}$ denote relevant four-fermion operators without derivatives and O_W the Weinberg operator.

Now, starting with the WCs of a top quark C_{tB} and C_{tW} that determine d_t and using the RG equations of the SMEFT and subsequently the ones of LEFT, one can determine the contribution of d_t to d_d and d_u and consequently to neutron electric dipole moment. The bounds on the latter imply the bounds on d_t. Similarly, the nonvanishing coefficients $C_{\tau B}$ and $C_{\tau W}$ that determine d_τ can have impact not only on the electron EDM d_e but also on $d_{d,u}$. The bounds on $d_{e,d,u}$ imply then the bounds on d_τ.

As an example we quote one-loop contributions to electric and weak dipole moments of d-quark and u-quark at the electroweak scale μ_{EW} ($t_W = \tan \vartheta_W$)

$$d_d^{\gamma} \supset \frac{\alpha}{16\pi \sin^2 \vartheta_W} \frac{m_d m_i}{M_W^2} |V_{id}|^2 \ln\left(\frac{\Lambda^2}{\mu_{EW}^2}\right) \left[\frac{1-t_W^2}{1+t_W^2} d_i^{\gamma} - \sin 2\vartheta_W d_i^Z \right], \; i = c, t, \tag{17.118}$$

$$d_d^{Z} \supset \frac{-\alpha}{16\pi \sin^2 \vartheta_W} \frac{m_d m_i}{M_W^2} |V_{id}|^2 \ln\left(\frac{\Lambda^2}{\mu_{EW}^2}\right) \left[\frac{1-t_W^2}{1+t_W^2} d_i^{Z} + \sin 2\vartheta_W d_i^{\gamma} \right], \; i = c, t, \tag{17.119}$$

$$d_u^{\gamma} \supset \frac{\alpha}{16\pi \sin^2 \vartheta_W} \frac{m_u m_i}{M_W^2} |V_{ui}|^2 \ln\left(\frac{\Lambda^2}{\mu_{EW}^2}\right) \left[\frac{1-t_W^2}{1+t_W^2} d_i^{\gamma} - \sin 2\vartheta_W d_d^Z \right], \; i = b, \tag{17.120}$$

$$d_u^{Z} \supset \frac{-\alpha}{16\pi \sin^2 \vartheta_W} \frac{m_u m_i}{M_W^2} |V_{ui}|^2 \ln\left(\frac{\Lambda^2}{\mu_{EW}^2}\right) \left[\frac{1-t_W^2}{1+t_W^2} d_i^{Z} + \sin 2\vartheta_W d_i^{\gamma} \right], \; i = b. \tag{17.121}$$

Calculating C_{fB} and C_{fW} for a given heavy fermion f as functions of fundamental parameters of a given theory and inserting them into (17.114) and (17.115) allows to calculate d_f^{γ} and d_f^Z of this fermion. Inserting the results into formulas just listed allows to calculate $d_{d,u}^{\gamma}$ and $d_{d,u}^Z$ as functions of these fundamental parameters and consequently neutron and proton EDMs, although the last step is tough because of theoretical uncertainties. Comparing the results with existing experimental bounds on the EDMs in question allows to put constraints on the fundamental parameters and consequently on the EDMs of heavy fermions.

On the other hand, the presence of operators $O_{\tau B}$ and $O_{\tau W}$ responsible for the d_τ cannot generate d_e, d_d, and d_u at one-loop level, but can do it via two-step RG running, discussed in Section 14.4, resulting in two-loop contributions to d_e, d_d, and d_u. The results for the imaginary parts of the relevant coefficients C_{fB} and C_{fW} with $f = e, d, u$ can be obtained using the technology outlined in Appendix E together with the RGE of [758–760]. We just

Downloaded from https://www.cambridge.org/core. UNIVERSIDAD AUTONOMA METROPOLITANA, on 16 Nov 2026 at 21:17:32, subject to the Cambridge Core terms of use, available at https://www.cambridge.org/core/terms. https://doi.org/10.1017/9781139524100.023

give the final results in the approximations made in Appendix E. More accurate numerical results are given in our paper, which should appear in hep-arxiv in 2020.

We find then

$$\mathrm{Im}(C_{eB}) = F_e \left[\left(\frac{3}{2} g_2^2 + 4 g_1^2 \bar{y}_e^2 \right) \mathrm{Im}(C_{\tau B}) + 3 g_1 g_2 \bar{y}_e \mathrm{Im}(C_{\tau W}) \right], \tag{17.122}$$

$$\mathrm{Im}(C_{eW}) = F_e \left[(g_2^2 + 2 g_1^2 \bar{y}_e^2) \mathrm{Im}(C_{\tau W}) + g_1 g_2 \bar{y}_e \mathrm{Im}(C_{\tau B}) \right], \tag{17.123}$$

$$\mathrm{Im}(C_{dB}) = F_d \left[\left(\frac{3}{2} g_2^2 + 4 g_1^2 \bar{y}_e \bar{y}_d \right) \mathrm{Im}(C_{\tau B}) + 3 g_1 g_2 \bar{y}_e \mathrm{Im}(C_{\tau W}) \right], \tag{17.124}$$

$$\mathrm{Im}(C_{dW}) = F_d \left[(g_2^2 + 2 g_1^2 \bar{y}_e \bar{y}_d) \mathrm{Im}(C_{\tau W}) + g_1 g_2 \bar{y}_d \mathrm{Im}(C_{\tau B}) \right], \tag{17.125}$$

$$\mathrm{Im}(C_{uB}) = F_u \left[\left(-\frac{3}{2} g_2^2 + 6 g_1^2 \bar{y}_e \bar{y}_u \right) \mathrm{Im}(C_{\tau B}) - 6 g_1 g_2 \bar{y}_e \mathrm{Im}(C_{\tau W}) \right], \tag{17.126}$$

$$\mathrm{Im}(C_{uW}) = F_u \left[\left(\frac{5}{2} g_2^2 - 2 g_1^2 \bar{y}_e \bar{y}_u \right) \mathrm{Im}(C_{\tau W}) - 2 g_1 g_2 \bar{y}_u \mathrm{Im}(C_{\tau B}) \right], \tag{17.127}$$

where

$$F_i = 2 \frac{m_i m_\tau}{v^2} \left[\frac{1}{16\pi^2} \ln \left(\frac{\Lambda}{\mu} \right) \right]^2, \qquad \bar{y}_f = \begin{cases} (Y_q + Y_f) \text{ for } f = u, d \\ (Y_l + Y_f) \text{ for } f = e \end{cases}. \tag{17.128}$$

Here Y_k are the hypercharges, that is $Y_q = 1/6$, $Y_l = -1/2$, $Y_e = -1$, $Y_d = -1/3$, and $Y_u = 2/3$.

With these formulas at hand one can not only get bounds on d_τ^γ and d_τ^Z but also include two-loop effects in the calculations of $d_{d,u}^\gamma$ and $d_{d,u}^Z$ generated by τ's EDMs. Moreover, now d_e^γ and d_e^Z enter the analysis providing additional constraints on NP.

The only important three-loop contribution is a contribution to the light-fermion EDMs via diagrams analogous to the light-by-light contributions to $(g-2)_\mu$ [1225]. The key property of these diagrams is that the only relevant mass scales are the fermion masses. In the case of a mass hierarchy between the intermediate and external fermions F and f, dimensional analysis implies $d_f \sim m_f/m_F (\alpha/\pi)^3$. In the case of fermions with intermediate masses (like the charm quark) this mechanism can be competitive to the one- and two-loop contributions.

We can now return to Table 17.8. It illustrates the scaling of contributions of the CP-violating dipole moments of light fermions in terms of those of heavier ones, displaying explicitly loop factors, fermion and gauge boson masses, gauge couplings, electric charges, the number of colors, $N_C = 3$, and potentially large logarithms. The various hierarchies involved complicate the identification of the dominant contributions for a given fermion. Yet, some properties are evident:

- d_e does not receive any one-loop contributions,
- $d_{\mu,\tau}$ do not contribute to d_e, d_d, d_u at one-loop level,
- The only one-loop contributions are present in the generation of d_d from $d_{U=(c),t}$ and of d_u from $d_{D=(s),b}$
- All entries in the table that involve two- and three-loop contributions are nonvanishing.

Downloaded from https://www.cambridge.org/core. UNIVERSIDAD AUTONOMA METROPOLITANA, on 16 Nov 2026 at 21:17:32, subject to the Cambridge Core terms of use, available at https://www.cambridge.org/core/terms. https://doi.org/10.1017/9781139524100.023

Table 17.8 Scaling for contributions at one, two, and three loops (first, second, and third line of each entry) to the light fermion EDMs.

	$d_{U=(c),t}$	$d_{D=(s),b}$	$d_{L=(\mu),\tau}$
	—	—	—
d_e	$\frac{m_e m_U G_F}{(4\pi)^2}\frac{\alpha}{\pi}\frac{N_C}{\tan^2\vartheta_W}\ln^2\left(\frac{\Lambda}{\mu_{EW}}\right)$	$\frac{m_e m_D G_F}{(4\pi)^2}\frac{\alpha}{\pi}\frac{N_C}{\tan^2\vartheta_W}\ln^2\left(\frac{\Lambda}{\mu_{EW}}\right)$	$\frac{m_e m_L G_F}{(4\pi)^2}\frac{\alpha}{\pi}\frac{1}{\tan^2\vartheta_W}\ln^2\left(\frac{\Lambda}{\mu_{EW}}\right)$
	$\frac{m_e}{m_U}q_U^3\left(\frac{\alpha}{\pi}\right)^3 N_C$	$\frac{m_e}{m_D}q_D^3\left(\frac{\alpha}{\pi}\right)^3 N_C$	$\frac{m_e}{m_L}\left(\frac{\alpha}{\pi}\right)^3$
	$\frac{m_d m_U G_F}{(4\pi)^2}\lvert V_{Ud}\rvert^2\ln\left(\frac{\Lambda}{\mu_{EW}}\right)$	—	—
d_d	$\frac{m_d m_U G_F}{(4\pi)^2}\frac{\alpha}{\pi}\frac{N_C}{\tan^2\vartheta_W}\ln^2\left(\frac{\Lambda}{\mu_{EW}}\right)$	$\frac{m_d m_D G_F}{(4\pi)^2}\frac{\alpha}{\pi}\frac{N_C}{\tan^2\vartheta_W}\ln^2\left(\frac{\Lambda}{\mu_{EW}}\right)$	$\frac{m_d m_L G_F}{(4\pi)^2}\frac{\alpha}{\pi}\frac{1}{\tan^2\vartheta_W}\ln^2\left(\frac{\Lambda}{\mu_{EW}}\right)$
	$\frac{m_d}{m_U}q_U^3 q_d^3\left(\frac{\alpha}{\pi}\right)^3 N_C$	$\frac{m_d}{m_D}q_D^3 q_d^3\left(\frac{\alpha}{\pi}\right)^3 N_C$	$\frac{m_d}{m_L}\left(\frac{\alpha}{\pi}\right)^3$
	—	$\frac{m_u m_D G_F}{(4\pi)^2}\lvert V_{uD}\rvert^2\ln\left(\frac{\Lambda}{\mu_{EW}}\right)$	—
d_u	$\frac{m_u m_U G_F}{(4\pi)^2}\frac{\alpha}{\pi}\frac{N_C}{\tan^2\vartheta_W}\ln^2\left(\frac{\Lambda}{\mu_{EW}}\right)$	$\frac{m_u m_D G_F}{(4\pi)^2}\frac{\alpha}{\pi}\frac{N_C}{\tan^2\vartheta_W}\ln^2\left(\frac{\Lambda}{\mu_{EW}}\right)$	$\frac{m_u m_L G_F}{(4\pi)^2}\frac{\alpha}{\pi}\frac{1}{\tan^2\vartheta_W}\ln^2\left(\frac{\Lambda}{\mu_{EW}}\right)$
	$\frac{m_u}{m_U}q_U^3 q_u^3\left(\frac{\alpha}{\pi}\right)^3 N_C$	$\frac{m_u}{m_D}q_D^3 q_u^3\left(\frac{\alpha}{\pi}\right)^3 N_C$	$\frac{m_u}{m_L}q_u^3\left(\frac{\alpha}{\pi}\right)^3$

- The hierarchies implied by the scalings in Table 17.8 are drastically different for the different flavors. For the top quark, the two-loop contributions are clearly dominant because the one-loop ones are suppressed by $|V_{td}|^2$ and the three-loop ones are not enhanced compared to $m_t^2/v^2 \sim 1$. On the other hand, for the charm quark, all three loop levels are comparable, despite each class receiving different suppression factors.

Numerical analysis of these formulas with the bounds on EDMs of heavy fermions should appear in hep-arxiv in 2020.

17.4 Anomalous Magnetic Moments $(g-2)_{\mu,e}$

17.4.1 Preliminaries

Although $a_{e,\mu}$ are both flavor- and CP-conserving, they also offer powerful probes to test the SM and its extensions. In particular the anomalous magnetic moment of the muon

$$\boxed{a_\mu = \frac{(g-2)_\mu}{2},} \tag{17.129}$$

which we defined in Section 17.1.3, provides an excellent test for physics beyond the SM.

Downloaded from https://www.cambridge.org/core. UNIVERSIDAD AUTONOMA METROPOLITANA, on 16 Nov 2026 at 21:17:32, subject to the Cambridge Core terms of use, available at https://www.cambridge.org/core/terms. https://doi.org/10.1017/9781139524100.023

On the theory side a_μ receives within the SM four dominant contributions:

$$a_\mu^{\rm SM} = a_\mu^{\rm QED} + a_\mu^{\rm ew} + a_\mu^{\gamma\gamma} + a_\mu^{\rm hvp}. \tag{17.130}$$

While the QED [1226–1229] and EW contributions [803, 1230] to $a_\mu^{\rm SM}$ are known very precisely and the light-by-light contribution $a_\mu^{\gamma\gamma}$ is currently known with a reasonable accuracy [1231, 1232], the theoretical uncertainty is dominated by the hadronic vacuum polarization. Review of the relevant calculations of all these contributions and references to related extensive analyses can be found in [803, 1119, 1233–1236].

The analyses by the master of this field, Fred Jegerlehner, just quoted, show that the very precise measurement of a_μ by the E821 experiment [1115] in Brookhaven,

$$a_\mu^{\rm exp} = (11659209.1 \pm 5.4 \pm 3.3[6.3]) \times 10^{-10}, \tag{17.131}$$

differs from its SM prediction by roughly 4σ

$$\boxed{a_\mu^{\rm exp} - a_\mu^{\rm SM} = (31.3 \pm 7.7) \times 10^{-10}.} \tag{17.132}$$

Many NP models have been used by many theorists with the goal to explain this discrepancy. Especially supersymmetric models were very popular [1237–1243] ten years ago. In SUSY the discrepancy could easily be accommodated for relatively light smuon masses and large $\tan\beta$. However, so far no light SUSY particles have been discovered. Another approach was followed in [1244], where the interplay of $(g-2)_\mu$ and a soft muon Yukawa coupling that is generated radiatively in the MSSM was studied. With the increased SUSY mass scale the explanation of $(g-2)_\mu$ anomaly became difficult already in 2012 [1245]. We will return to other extensions of the SM in this context.

On the experimental side, the $g-2$ ring at BNL has been disassembled and brought to Fermilab for a run, which started in 2017. The data are expected in 2020. An experiment at J-PARC should provide an independent measurement in the coming years.

The anomalous magnetic moment of the muon a_μ is more sensitive to lepton flavor-conserving NP than a_e, and consequently the latter was not as popular as a_μ until recently. However, as emphasized in [1123] and in references quoted therein, because of the fact that a_e is very precisely measured and very precisely calculated within the SM, it can also be used to probe NP, even if the theory agrees very well with experiment. Indeed, a_e plays a central role in QED because its precise measurement provides the best source of $\alpha_{\rm em}$ assuming the validity of QED [1246]. Conversely, one can use a value of $\alpha_{\rm em}$ from a less precise measurement and insert it into the theory prediction for a_e to probe NP. The 2007 calculation implied [1247]

$$a_e = 1\ 159\ 652\ 182.79\,(7.71) \times 10^{-12}, \tag{17.133}$$

where the largest uncertainty came from the second-best measurement of $\alpha_{\rm em}$, which is $\alpha_{\rm em}^{-1} = 137.03599884(91)$ from a Rubidium atom experiment [1248]. The difference between experiment and data turned out to be 1.7σ.

Downloaded from https://www.cambridge.org/core. UNIVERSIDAD AUTONOMA METROPOLITANA, on 16 Nov 2026 at 21:17:32, subject to the Cambridge Core terms of use, available at https://www.cambridge.org/core/terms. https://doi.org/10.1017/9781139524100.023

However, recently a measurement using atomic Cesium [1249] resulted in the new most precise value

$$\alpha_{\rm em}^{-1} = 137.035999046(27). \tag{17.134}$$

Comparison of the theoretical SM prediction for $a_e^{\rm SM}$ [1250] with the existing experimental measurement $a_e^{\rm exp}$ [1251] now leads to a discrepancy of 2.4 σ,

$$\boxed{\Delta a_e \equiv a_e^{\rm exp} - a_e^{\rm SM} = (-87 \pm 36) \times 10^{-14},} \tag{17.135}$$

with errors added in quadrature. I can recommend a very nice paper by Davoudiasl and Marciano [1252] that discusses the implications of this new anomaly. See also [1253], where a combined explanation of $(g-2)_{\mu,e}$ anomalies with implications for a large muon EDM has been presented.

In what follows we will collect one-loop formulas for a_μ, which allow to calculate the contribution to a_μ in any model with fermions, gauge bosons, and scalars. These formulas can easily be generalized to a_ℓ with $\ell = e, \tau$. Such formulas were first derived in [802] and subsequently by many authors. See, e.g., [803]. In particular systematic presentation of various cases has been done recently in [804]. Exact results in terms of integrals can be found both in [802] and [804].

Here we will confine our presentation to approximate formulas derived in [804] that have been verified by Robert Szafron. We should, however, stress that these formulas are listed here to primarily give the reader a rough idea on the structure of various contributions as functions of the involved masses and couplings. For phenomenology it is advisable to use exact expressions given in [802] and [804].

The contributing diagrams are given in Figure 17.4 with all particles being physical. Indeed, as there are no tree-level contributions, results of one-loop calculations must be finite so that even a nonrenormalizable gauge like unitary gauge can be used for calculations.

17.4.2 Gauge Boson Contributions

These are obtained from diagrams (a) and (b) in Figure 17.4, where F denotes any fermion and X a gauge boson with electric charges Q_F and Q_X, respectively. They will be given in units of $e > 0$ so that $Q_\mu = -1$. The interaction Lagrangian is given as

$$\mathcal{L}_{\rm int} = \sum_{F,X} \bar{F}_i [C_V^{ij}(X)\gamma^\mu + C_A^{ij}(X)\gamma^\mu\gamma^5] l_j X_\mu, \tag{17.136}$$

where $l_j = e, \mu, \tau$. The sum is over all fermions F including the SM fermions and over all gauge bosons X that also include SM gauge bosons. Model dependence enters through the coefficients C_V and C_A. In a given model they can be read off the interaction Lagrangian in the *unitary gauge*.

Downloaded from https://www.cambridge.org/core. UNIVERSIDAD AUTONOMA METROPOLITANA, on 16 Nov 2026 at 21:17:32, subject to the Cambridge Core terms of use, available at https://www.cambridge.org/core/terms. https://doi.org/10.1017/9781139524100.023

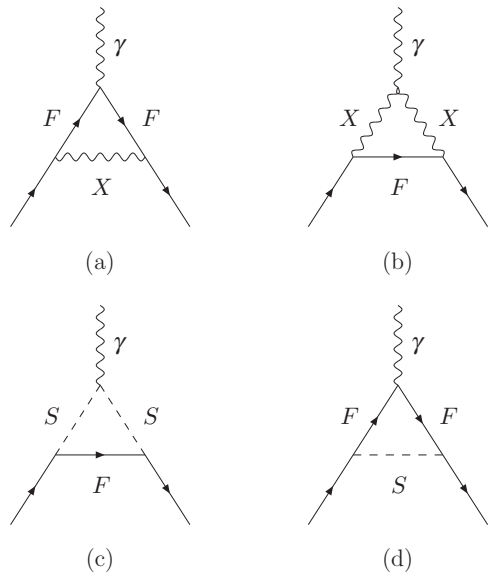


Figure 17.4 Diagrams contributing to $(g-2)_\mu$. F denotes a fermion, X a gauge boson, and S a scalar or pseudoscalar. The outgoing fermion is μ, but could also be e or τ.

The formulas listed following can easily be generalized to a_e and a_τ, but to avoid proliferation of the indices we will give all formulas for the case of the muon. Moreover, it is sufficient to expand in m_μ/M_X.

Charged Fermion and Neutral Gauge Boson

As a simple example we consider the case of a heavy neutral gauge boson Z' and a charged fermion $F_i = E_i$ with a mass m_{E_i}. In this case, with $Q_E = -1$ from charge conservation and $Q_X = Q_{Z'} = 0$, only the diagram (a) in Figure 17.4 contributes. For a Z' much heavier than μ and E_i one finds [804] ($C_V = \Delta_V/2$ and $C_A = \Delta_A/2$ in our notation)

$$\boxed{\Delta a_\mu(E_i, Z') \approx -\frac{1}{4\pi^2}\frac{m_\mu^2}{M_{Z'}^2}\left[\left|C_V^{i\mu}(Z')\right|^2\left(\frac{2}{3}-\frac{m_{E_i}}{m_\mu}\right)+\left|C_A^{i\mu}(Z')\right|^2\left(\frac{2}{3}+\frac{m_{E_i}}{m_\mu}\right)\right].} \tag{17.137}$$

Usually contributions from $E_i = e, \mu, \tau$ have to be added. If E_i is a new heavy lepton and $m_{E_i}/M_{Z'} \geq 0.2$, exact expressions in [804] have to be used.

In terms of Z' couplings used in this book

$$C_{V,A}^{ij}(Z') = \frac{1}{2}\Delta_{V,A}^{ij}(Z') = \frac{1}{2}\left[\Delta_R^{ij}(Z') \pm \Delta_L^{ij}(Z')\right], \tag{17.138}$$

see (15.54).

Downloaded from https://www.cambridge.org/core. UNIVERSIDAD AUTONOMA METROPOLITANA, on 16 Nov 2026 at 21:17:32, subject to the Cambridge Core terms of use, available at https://www.cambridge.org/core/terms. https://doi.org/10.1017/9781139524100.023

Neutral Fermion and Charged Gauge Boson

We consider next the case of a heavy charged gauge boson W' and a neutral fermion N_i with a mass m_{N_i}. In this case, with $Q_F = Q_N = 0$, only the diagram (b) in Figure 17.4 contributes. For W' much heavier than μ and N_i one finds [804]

$$\Delta a_\mu(N_i, W') \approx \frac{1}{4\pi^2}\frac{m_\mu^2}{M_{W'}^2}\left[\left|C_V^{i\mu}(W')\right|^2\left(\frac{5}{6}-\frac{m_{N_i}}{m_\mu}\right)+\left|C_A^{i\mu}(W')\right|^2\left(\frac{5}{6}+\frac{m_{N_i}}{m_\mu}\right)\right]. \tag{17.139}$$

As this simple formula works very well only for $m_{N_i}/M_{W'} \leq 0.3$, for a heavy N_i exact expressions in [804] have to be used.

17.4.3 Scalar Contributions

These are obtained from diagrams (c) and (d) in Figure 17.4, where F denotes any fermion and S a scalar or pseudoscalar with electric charges Q_F and Q_S

The interaction Lagrangian for a charged scalar S^+ and a neutral fermion N_i is given as follows

$$\mathcal{L}_{\text{Yukawa}} = \sum_{N,S} S^+ \bar{N}_i [C_S^{ij}(S^+) + C_P^{ij}(S^+)\gamma^5] l_j, \tag{17.140}$$

where again $l_j = e, \mu, \tau$. In the case of a neutral scalar S^0 and a charged fermion E_i we have

$$\mathcal{L}_{\text{Yukawa}} = \sum_{E,S} S^0 \bar{E}_i [C_S^{ij}(S^0) + C_P^{ij}(S^0)\gamma^5] l_j, \tag{17.141}$$

where again $l_j = e, \mu, \tau$.

The sum is over all fermions $F = N, E$ that is also the SM fermions and over all scalars and pseudoscalars S that is also Higgs scalar. Model dependence enters through the coefficients C_S and C_P. In a given model they can be read off the interaction Lagrangian in the unitary gauge.

Neutral Fermion and Charged Scalar

As a simple application we consider the case of a heavy charged scalar S^+ and a neutral fermion N_i with a mass m_{N_i}. In this case, with $Q_F = Q_{N_i} = 0$, only diagram (c) in Figure 17.4 contributes. For S^+ much heavier than μ and N_i one finds [804]

$$\Delta a_\mu(N_i, S^+) \approx -\frac{1}{4\pi^2}\frac{m_\mu^2}{M_{S^+}^2}\left[|C_S(S^+)|^2\left(\frac{1}{12}+\frac{m_{N_i}}{4m_\mu}\right)+|C_P(S^+)|^2\left(\frac{1}{12}-\frac{m_{N_i}}{4m_\mu}\right)\right]. \tag{17.142}$$

Downloaded from https://www.cambridge.org/core. UNIVERSIDAD AUTONOMA METROPOLITANA, on 16 Nov 2026 at 21:17:32, subject to the Cambridge Core terms of use, available at https://www.cambridge.org/core/terms. https://doi.org/10.1017/9781139524100.023

Exact result in terms of integrals can be found both in [802] and [804]. It turns out that the preceding simple formula works very well only for $m_{N_i}/M_{S^+} \leq 0.1$.

Charged Fermion and Neutral Scalar

Finally, we consider the case of a heavy neutral scalar S^0 and a charged fermion E_i with a mass m_{E_i}. In this case, with $Q_F = Q_E = -1$ and $Q_S = 0$, only diagram (d) in Figure 17.4 contributes. For S^0 much heavier than μ and E_i one finds [804]

$$\boxed{\Delta a_\mu(E_i, S^0) \approx \frac{1}{4\pi^2}\frac{m_\mu^2}{M_{S^0}^2}\left[|C_S(S^0)|^2\left(\frac{1}{6} - \frac{m_{E_i}}{m_\mu}P\right) + |C_P(S^0)|^2\left(\frac{1}{6} + \frac{m_{E_i}}{m_\mu}P\right)\right],} \tag{17.143}$$

with

$$P = \frac{3}{4} + \ln\left(\frac{m_E}{m_S}\right). \tag{17.144}$$

Again exact results in terms of integrals can be found both in [802] and [804]. It turns out that the preceding simple formula works very well only for $m_{E_i}/M_{S^0} \leq 0.1$.

17.4.4 Beyond the SM

With these formulas at hand one can study basically all extensions of the SM that contain new heavy fermions, new heavy gauge bosons, and new heavy scalars. A very nice review in this context is the one in [804] in which $(g-2)_\mu$ in numerous simplified models and concrete models with UV completions has been analyzed in detail. In addition to examples presented here also examples with doubly charged scalars, fermions, and gauge bosons present in some extensions of the SM have been considered. In particular correlations between $(g-2)_\mu$ and $\mu \to e\gamma$ and also $\mu \to 3e$ have been analyzed in these models in detail. I can strongly recommend this review as it is very systematically written and contains over 500 references, which certainly will motivate the readers to learn more about this subject. In particular, the desire to explain the $(g-2)_\mu$ anomaly led various authors to invoke vector-like leptons. See, e.g., [943, 1034–1038] and references therein. Prospects for vector-like leptons at future proton-proton colliders are reviewed in [1254], where further references to theoretical papers can be found. This review indicates that vector-like leptons with masses above 10 TeV will be probed only by indirect searches even in the presence of a 100 TeV collider. The explanation of a_μ and a_e anomalies with the help of axion-like particles has been suggested in [1315].

For me the main messages from all these studies is the following one: Provided the $(g-2)_\mu$ anomaly will be confirmed by the Fermilab experiment, we will have fun, using the expressions and plots in [804] and other papers listed earlier, to find out which mediators are hiding behind this anomaly. But simultaneously one should look at correlations with other processes considered in this book.

Downloaded from https://www.cambridge.org/core. UNIVERSIDAD AUTONOMA METROPOLITANA, on 16 Nov 2026 at 21:17:32, subject to the Cambridge Core terms of use, available at https://www.cambridge.org/core/terms. https://doi.org/10.1017/9781139524100.023

Last, but certainly not least, the formfactors listed in Table 17.4 for $f = i$ can be directly used to calculate NP contributions to anomalous magnetic moments of charged leptons [795]

$$\boxed{a_{l_i} = \frac{2m_{l_i}}{e\Lambda^2}\mathrm{Re}[F_{TR}^{ii}].} \tag{17.145}$$

17.5 Neutrino Oscillations

The observation of neutrino oscillations is a clear signal of physics beyond the SM and so far together with Dark Matter and the matter-antimatter asymmetry observed in our universe the only clear sign of NP.

To accommodate neutrino masses one needs to extend the SM. The most straightforward way is to proceed in the same manner as for quark and charged lepton masses and just introduce three right-handed neutrinos that are singlets under the SM gauge group anyway. A Dirac mass term is then generated via the usual Higgs coupling $\bar{\nu}_L Y_\nu H \nu_R$. However, then there is also the possibility for a Majorana mass term for the right-handed neutrinos because it is gauge invariant. One would need to introduce or postulate a further symmetry to forbid this term, which is also already an extension of the SM. Furthermore, this Majorana mass term introduces an additional scale M_R and because it is not protected by any symmetry it could be rather high. Then with the help of the so-called seesaw mechanism one can generate light neutrino masses as observed in nature. Another possibility to get neutrino masses without right-handed neutrinos is the introduction of an additional Higgs-triplet field. Either way, the accommodation of neutrino masses requires an extension of the SM.

Here, in addition to CP-violation in the lepton sector, which has not been discovered yet, neutrinoless double-beta decay plays a very prominent role. It will tell us whether a neutrino is a Dirac or Majorana particle. All these topics are very important. Unfortunately the author of this book never explored this valley of NP and can only direct interested readers to the excellent textbook by Bilenky [23] on massive neutrino physics and most recent reviews and papers on the neutrinoless double-beta decay [797, 1255–1258]. Finally, I enjoyed very much the history of neutrino masses and mixing presented in [1259].

Downloaded from https://www.cambridge.org/core. UNIVERSIDAD AUTONOMA METROPOLITANA, on 16 Nov 2026 at 21:17:32, subject to the Cambridge Core terms of use, available at https://www.cambridge.org/core/terms. https://doi.org/10.1017/9781139524100.023